HHS Public Access

Author manuscript

Neurobiol Dis. Author manuscript; available in PMC 2021 January 29.

Published in final edited form as:

Neurobiol Dis. 2021 January ; 148: 105221. doi:10.1016/j.nbd.2020.105221.

Changes in the brain transcriptome after DNA Aβ42 trimer immunization in a 3xTg-AD mouse model

Doris Lambracht-Washington[a,c,*], **Min Fu**[a], **Linda S. Hynan**[b], **Roger N. Rosenberg**[a]

[a]Department of Neurology, UT Southwestern Medical Center Dallas, USA

[b]Departments of Population and Data Sciences (Biostatistics) & Psychiatry, UT Southwestern Medical Center Dallas, USA

[c]Doris Lambracht Washington, UT Southwestern Medical Center Dallas, Department of Neurology , 5323 Harry Hines Blvd, Dallas, TX 75390-8813, USA

Abstract

Alzheimer's disease (AD) has been associated with accumulation of amyloid beta (Aβ) peptides in brain, and immunotherapy targeting Aβ provides potential for AD prevention. We have used a DNA Aβ42 trimer construct for immunization of 3xTg-AD mice and found previously significant reduction of amyloid and tau pathology due to the immunotherapy. We show here that DNA Aβ42 immunized 3xTg-AD mice showed better performance in nest building activities and had a higher 24 months survival rate compared to the non-treated AD controls. The analysis of differently expressed genes in brains from 24 months old mice showed significant increases transcript levels between non-immunized AD mice and wild-type controls for genes involved in microglia and astrocyte function, cytokine and inflammatory signaling, apoptosis, the innate and adaptive immune response and are consistent with an inflammatory phenotype in AD. Most of these upregulated genes were downregulated in the DNA Aβ42 immunized 3xTg-AD mice due to the vaccine. Transcript numbers for the immediate early genes, *Arc, Bdnf, Homer1, Egr1* and *cfos*, involved in neuronal and neurotransmission pathways which were much lower in the non-immunized 3xTg-AD mice, were restored to wild-type mouse brain levels in DNA Aβ42 immunized 3xTg-AD mice indicating positive effects of DNA Aβ42 immunotherapy on synapse stability and plasticity. The immune response after immunization is complex, but the multitude of changes after DNA Aβ42 immunization shows that this response moves beyond the amyloid hypothesis and into direction of disease prevention.

[*]Corresponding author at: Doris Lambracht Washington, UT Southwestern Medical Center Dallas, Department of Neurology and Neurotherapeutics, 5323 Harry Hines Blvd, Dallas, TX 75390-8813, USA., doris.lambracht-washington@utsouthwestern.edu (D. Lambracht-Washington).

Author statement

All authors have read the manuscript and agree to possible publication in the journal Neurobiology of Disease. All authors have no financial interests to declare.

DLW planned the experiments, performed the experiments, analyzed the data, wrote and revised the manuscript, MF performed the experiments, read the manuscript, revised the manuscript, LH read the revised manuscript, discussed the statistical necessities and performed statistical calculations to improve the data presentations, RNR planned the experiments, discussed the results, reviewed and edited the manuscript.

Supplementary data to this article can be found online at https://doi.org/10.1016/j.nbd.2020.105221.

Declaration of Competing Interest

None.

1. Introduction

Aβ42 immunotherapy is an ongoing area of research to find a treatment option to prevent progression of Alzheimer's disease in human patients. Active immunization for AD is currently an active area of neurotherapeutics: Three Aβ42 peptide immunogens, CAD106, ACC-001, and UB-311, are being evaluated in Phase 1 and 2 clinical trials (Hull et al., 2017; Pasquier et al., 2016; Vandenberghe et al., 2016; Wang et al., 2017; Winblad et al., 2012), and epitope based DNA vaccines, AV-1955 and YM3711, which have major sequence differences from our vaccine as they detect only short Aβ epitopes and are thus similar to the passive immunization therapies, are also being tested in pre-clinical studies (Evans et al., 2014; Matsumoto et al., 2013). It is important to note that treatment needs to go beyond the amyloid hypothesis (Hardy and Selkoe, 2002; Selkoe and Hardy, 2016; Karran and De Strooper, 2016; Makin, 2018; Schilling et al., 2018; Selkoe, 2019) to be successful. The DNA Aβ42 trimer vaccine presented here shows in the mouse AD model that it "goes beyond" amyloid by preventing amyloid and tau pathology, by reducing inflammation, and by inducing further changes which resulted in transcriptional changes of genes in AD mouse brain tissue.

We started over fifteen years ago to develop an anti-Aβ42 DNA vaccine to bias the immune response to Th2 and prevent the Th1 inflammatory immune responses found in the first clinical trial AN1792 in human AD patients with Aβ42 peptide immunizations (Orgogozo et al., 2003; Fox et al., 2005; Gilman et al., 2005; Lambracht-Washington et al., 2009; Rosenberg and Lambracht-Washington, 2020). The vaccine used here consists of an Aβ42 plasmid encoding three copies of the full-length Aβ42 sequence (Aβ1–42 x Aβ1–42 x Aβ1–42, 3× Aβ42, Aβ42 trimer) and was delivered into the skin of the mouse ears via gene gun administration (Qu et al., 2010). As shown previously in a group of 20 months old 3xTg-AD mice, which carries the human genes for APP with the Swedish mutation, MAPT with the P30IL mutation, and PS1 with the M146V mutation, DNA Aβ42 immunization reduced amyloid and tau pathology and was non-inflammatory (Rosenberg et al., 2018). We present here new data showing clinical benefits of DNA Aβ42 immunotherapy in regard to an improved nest building activities and higher 24-month survival rates compared to the non-treated AD control mice and Aβ42 peptide immunized mice. Furthermore, we present here for the first time data showing a multitude of changes in gene expression profiles in brain tissue from DNA Aβ42 trimer immunized 3xTg-AD mice compared to non-treated 3xTg-AD controls in genes important for the inflammatory response in AD (Akiyama et al., 2000), genes classified as AD associated (Naj et al., 2014; Rosenberg et al., 2016)), genes involved in transmitter vesicle formation and release (Parodi et al., 2010; Saura et al., 2015; Ovsepian et al., 2018; Chakroborty et al., 2019), and last but not least key genes of the immediate-early response after neuronal stimulation (Dickey et al., 2003; Hendrickx et al., 2014; Shepherd and Bear, 2011; Tyssowski et al., 2018). The transcriptome changes presented here are in accordance with the reports by others that inflammation is a major driver of pathology at late disease stages (Manavalan et al., 2013; Landel et al., 2014; Castillo et al., 2017).

2. Methods

2.1. Animals

3xTg-AD (B6/129-Psen1 Tg(APPSwe,tauP301L)1Lfa/Mmjax, APP^{swe}PS1MAPT) mice had been purchased from the Mutant Mouse Research and Resource Center (MMRRC) at JAX, and were bred and housed at the UTSouthwestern Medical Center Animal facility under conventional conditions. This mouse model had been developed by Oddo and colleagues (Oddo et al. 2003). Animal use was approved by the UT Southwestern Medical Center Animal Research Committee, and animal research was conducted under the ARRIVE guidelines (Kilkenny et al. 2010).

2.2. Mice and immunizations

Groups of female 3xTg-AD mice and female B6/129 F2 wild-type controls (n = 10–15/group) were immunized for a total of twelve times with DNA Aβ42 trimer using gene gun delivery over a time frame of 24 months. Control mice received Aβ1–42 peptide immunizations (100 μg peptide plus QuilA adjuvant, i.p.injections) or were left untreated. The DNA plasmids and immunization with the gene gun had been described previously in detail (Qu et al., 2010; Rosenberg et al., 2018), Immunizations were started in four months old mice in groups of ten to fifteen mice (3xTg-AD and B6129/SvJ wild-type controls) with three initial immunizations in biweekly intervals via i.p. injections of Aβ1–42 peptide (100 μg peptide/immunization) with QuilA as adjuvant. The immunizations were boosted in six week intervals until the mice were 24 months old. Control mice received no treatment (naïve controls). No immunizations were performed during or close to the behavior studies to avoid behavioral variances due to stress. Blood samples were collected at different time points throughout the study 10 days following the respective immunization time points.

2.3. Nesting behavior

Mice were placed individually in fresh cages, in which 6 g of shredded paper were dispersed throughout the cage. Pictures were taken after 24 h and scored on a scale of 1–5. A score of 1 represented no nest constructed and 5 represented a fully formed nest, with all of the paper in the cage being gathered tightly in one area (Suppl. Fig. 1).

2.4. ELISAs

Antibody concentrations in plasma were measured with standard ELISA assays and determined as μg anti-Aβ42 IgG/ml plasma. Plates were coated with Aβ1–42 peptide (rPeptide) at concentrations of 2 μg/ml diluted in coating buffer. As standard antibody the mouse monoclonal anti-Aβ17–24 IgG antibody 4G8 (Biolegend, San Diego, CA) was used. Antibody binding to Aβ42 peptide in the plates were measured with HRP conjugated anti-mouse IgG secondary antibody (Jackson Immunoresearch laboratories, West Grove, PA), TMB detection and measurement of optical density (OD) with an ELISA plate reader.

2.5. IFNγ and IL-17 FluoroSpots

FluoroSpot assays to determine frequencies of cytokine secreting cells were performed according to standard procedures and as previously described using commercial available

antibody sets for mouse IFNγ, IL-17, and IL-4 (Maptech, San Diego, CA, USA) (Lambracht-Washington et al., 2011; Lambracht-Washington and Rosenberg, 2015). 2.5 × 10^5 splenocytes were added per well and were cultured in medium only, or re-stimulated with Aβ42 peptides (10 μg/ml), and incubated at 37 °C in a 5% CO2 humidified incubator for 48 h. For maximal T cell stimulation an anti-CD3ε antibody (clone 145–2C11, eBioscience, Tonbo) was used at 0.5 μg/ml in the cell cultures. Spots were counted by a FluoroSpot plate reader service (Zellnet consulting, Fort Lee, NJ).

2.6. Memory T cell FluoroSPOT

Splenocytes from immunized and non-immunized mice were cultured for 10 days with and without Aβ42 antigen stimulation and IL-2 supplementation (10 ng/ml) at Day 3 and Day 7 of cell culture. On day 10, cells were harvested and plated onto pre-coated IFNγ FluoroSPOT plates and re-stimulated overnight with full-length Aβ1–42 peptide, and the shorter peptide Aβ10–26 (10^6 cells/well). IFNγ secreting cells (spots) were detected with a biotinylated anti-IFNγ antibody and visualized with AF550. Plates were read by a commercial plate reader service (Zellnet).

2.7. Immunohistochemistry of mouse brains

Mice were overdosed with avertin and perfused transcardially with cold PBS. Brains were extracted from the skulls and kept in 10% formalin at 4 °C for 48 h prior to further processing and paraffin embedding. Sagittal parallel sections of mouse brains were stained with antibodies specific for Aβ1–42 (6E10, Biolegend, San Diego CA, D-17, Santa Cruz Biotechnology, Dallas TX, McSA1, Medimabs, Canada) to detect intraneuronal Aβ42 deposition and amyloid plaques in hippocampus and cortex of the mice. HT7 and 43D antibodies (Thermofisher, Waltham MA, Biolegend) were used to stain for tangle pathology. NeuN antibodies (clones ABN78, Millipore and 1B7, abcam) were used to stain neurons. Prior to the staining sections were treated with heat-mediated antigen retrieval for the tau antibodies or incubation in 70% formic acid for Aβ antibodies. After staining, tissues were scanned using a Nano-Zoomer digital pathology system and analyzed with NDP viewer software (Hamamatzu, Japan), or an Axioscan system and Zen lite software (Zeiss, Germany).

2.8. Gene expression profiling from 3xTg-AD mouse brains which have received DNA Aβ1–42 trimer immunotherapy and non-treated control mice and comparison to age and gender matched wild-type mouse brains

A method developed by nanoString (Seattle, WA) enables the characterization of 750 to 800 RNA targets in a single assay. The included analysis of housekeeping genes and other positive controls as internal controls allows for signal normalization. Probe sets consist of two gene specific oligonucleotides: a capture probe and a reporter probe which both bind to the single gene they are designed for. After RNA/probe hybridization, the mixture was purified by several washing steps to remove unbound probes, before immobilization of the samples to a nCounter® cartridge from which the reporter probes was read using the nCounter® Digital Analyzer (available at the UTSouthwestern Core facilities). It provides a cost-effective solution for multiplex analysis of differently expressed gene of 12 to 24 samples in a single assay. It works without Reverse transcription of the RNA or any other

further amplification procedure, so that results counted represent a 1:1 ratio of the molecules found in the particular samples. The method has been shown to be highly reliable and robust for RNA samples isolated from Formalin Fixed Paraffin Embedded (FFPE) tissue samples such as mouse brain samples which are available from a large number of previous experiments in our laboratory as archived probes (Reis et al., 2011; Chen et al., 2016). Twelve mouse brains from three different groups of 24 months old mice (n = 4.group) were selected for the gene expression analyzes. Transcript numbers obtained in the nanoString assays were normalized against a panel of housekeeping genes and other controls using the basic nSolver® software package 4.0 (nanoString Technologies) prior to all analyzes described in the results sections.

The Neuroinflammation gene panel assay was run twice with the same RNA samples (n = 4 mouse brain sections/group), and the mouse AD gene panel was run once after that using the same RNA samples.

2.9. Statistical analyses

GraphPad Prism 6.02 and IBM SPSS v26 were used to analyze and plot the data in bar graphs. Data normalization for gene expressions was performed using the nSolver Analysis Software 4.0. Statistical differences between three or more unmatched groups were assessed using the Kruskal-Wallis test and when significant followed with Dunn's post hoc multiple comparisons test. Differences between two groups of samples were analyzed using the Wilcoxon rank sum test or Mann-Whitney U test. Data analyzed using non-parametric tests are shown as median ± semi interquartile range (SIQR). Non-parametric analyses were conducted since the number of cases in each group for the continuous measures was too small to assume the data were normally distributed. Significance was set at $p < 0.05$. No adjustments for multiple testing have been performed. Ratio data were graphed using a log2 transformation to make the values linear.

2.10. Expression Heat maps and Volcano plots

Gene expression heat maps were constructed from log2 ratio expression differences compared to the wild-type mouse brain values using the CA heat mapper program (www.heatmapper.ca/expression) with average linkage as clustering method and Spearman Rank Correlation as distance measuring method. Identical colors and shades were applied to all the maps shown.

A volcano plot is a scatter-plot used to identify changes in large data sets of replicates (Li et al., 2014). Each point represents a gene with the x-axis showing the magnitude of the change (log fold change) and the y-axis showing the statistical significance (log10 of the p value from a t-test). These plots are helpful in genomics experiments containing thousands of replicate data points between two conditions to identify the most meaningful changes. Data points with low p values (highly significant) appearing towards the top of the plot. The x-axis is the log of the fold change between the two conditions. Data points on the right hand side represent downregulated genes in the comparison of the two groups. Data points on the left hand side are upregulated, respectively. Volcano plots were calculated with the Advanced Analysis Module of the nSolver Software. Raw count values were used in this

assay as the Advanced Analysis Module uses a different algorithm for data normalization and log2 ratio difference calculation (Waggott et al., 2012).

2.11. Survival Rates in 24 months old mice

A Kaplan Meier Survival curve was generated using Graphpad Prism 6.02 for the four groups of mice: Non-immunized 3xTg-AD controls, DNA Aβ42 immunized 3xTg-AD mice, Aβ42 peptide immunized mice, and age and gender matched wild-type controls (B6129F2 females).

3. Results

3.1. Nesting activity is improved in DNA Aβ42 trimer immunized 3xTg-AD mice

The natural behavior of nest building in mice has been used to assess impairment in mice with amyloid and tau pathologies and can be quantified based on scores (Torres-Lista and Giménez-Llort, 2013; Boeddrich et al., 2019; Samaey et al., 2019). Compared to non-treated or Aβ1–42 peptide ($n = 3$, nesting score of 4 ± 1) immunized and non-immunized 3xTg-AD female mice ($n = 10$, nesting score of 3 ± 1), the DNA Aβ42 trimer immunized mice ($n = 8$) exhibited higher nesting scores (4 ± 0, Suppl. Fig. 1, Fig. 1A). B6129F2 ($n = 14$) female wildtype mice had nesting scores of 5 ± 2. Comparative analysis of all groups using the Kruskal-Wallis test did not show statistical significance between the groups ($p = 0.30$).

3.2. Increased life span in DNA Aβ42 immunized 3xTg-AD mice

At the end of the experimental time line of 24 months, 77% of the original female wild-type mice (7 of 9) were still alive; from 15 DNA Aβ42 immunized female 3xTg-AD mice 64% (9 of 15) were alive after 24 months, from the female 3xTg-AD control mice which were left untreated 45% were alive at 24 months of age (9 of 20), and from the female Aβ42 peptide immunized only 2 of 11 mice were still alive at 24 months of age (18%, Fig. 1B). The survival curves were significantly different ($p = 0.0305$, Log-rank (Mantel-Cox) test).

3.3. Anti-Aβ antibodies in the immunized mice

Kruskal-Wallis statistical analysis was significant for the difference in antibody levels between the groups (p value <0.0001, Fig. 2A). The DNA Aβ42 trimer immunized 3xTg-AD mice (n = 8) in the 24 months old cohort had anti-Aβ42 IgG antibodies levels of 50.54 ± 13.14 μg/ml plasma (median ± SIQR). DNA Aβ42 immunized B6129F2 wildtype ($n = 5$) mice had non-significantly higher anti-Aβ42 antibody levels of 84.27 ± 9.91 μg/ml plasma. Antibody levels in Aβ1–42 peptide immunized mice ($n = 3$) were significantly higher with 333.9 ± 1.5 μg/ml plasma (p value 0.0059 Dunn's post hoc test). Plasma samples had been tested in a 1:500 dilution.

3.4. No IFNγ and IL-17 secretion in re-stimulated splenocytes from DNA Aβ42 immunized 3xTg-AD mice

Consistent with our previous findings, no inflammatory immune responses were detected the 24 months old 3xTg-AD mice which had received DNA Aβ42 immunizations in splenocytes cultures which were re-stimulated with Aβ42 peptide while splenocytes from the mice

which had received Aβ42 peptide immunizations showed high numbers of IFNγ and IL-17 producing cells in the respective FluoroSpot assays (Fig. 2B and C). For the inflammatory cytokine IFNγ, Aβ42 peptide immunized 3xTg-AD mice had 383.5 ± 115.5 (median ± SIQR) positive spots in the Aβ42 peptide re-stimulated wells (2 ± 0.5 spots in the medium controls, $p = 0.0238$, Mann-Whitney U test), while splenocytes from DNA Aβ42 trimer immunized mice did not produce IFNγ after Aβ42 peptide re-stimulation in culture. For the second inflammatory cytokine tested, IL-17, 3xTg-AD control mice had 36 ± 23.5 (median ± SIQR) IL-17 secreting cells per 2.5×10^5 splenocytes in the medium control wells and 73 ± 42.5 spots after Aβ42 peptide re-stimulation while Aβ42 peptide immunized mice showed 58 ± 6 IL-17 spots in the control wells and 508 ± 98 spots after Aβ42 peptide re-stimulation ($p = 0.0238$, Mann-Whitney U test). DNA Aβ42 trimer immunized mice did not show significant increased numbers of IL-17 spots after Aβ42 peptide re-stimulation in-vitro with 20 ± 8.5 spots in the control wells and 91 ± 4.5 spots after Aβ42 peptide re-stimulation ($p = 0.1$, Mann-Whitney U test, Fig. 2C).

Furthermore, no inflammatory T cell memory was detected in the DNA immunized mice while Aβ42 peptide immunized cells had high numbers of IFNγ producing memory T cells (Fig. 2D). Splenocytes from the non-immunized 3xTg-AD mice produced 50 ± 4.75 (median ± SIQR) spots in the medium control wells and 102 ± 12.5 spots in the wells with Aβ42 peptide (p value 0.0286 Mann-Whitney U test); splenocytes from Aβ42 peptide immunized 3xTg-AD mice produced 81.5 ± 18.62 spots in the medium control wells and 324 ± 34.25 spots after re-stimulation with Aβ42 peptide for 10 days (p value <0.0286 Mann-Whitney U test); splenocytes from DNA Aβ42 trimer immunized 3xTg-AD mice showed 160 ± 31.65 spots in the control wells and 154.5 ± 5.85 spots in the wells with Aβ42 peptide (p value 0.8857 Mann-Whitney U test).

3.5. DNA Aβ42 immunotherapy changed the gene expression profile in brain in the 3xTg-AD mouse

Parallel sagittal brain sections to the selected Formalin Fixed Paraffin Embedded (FFPE) sections from DNA Aβ42 immunized 3xTg-AD mice and the non-treated 3xTg-AD controls used for RNA isolation and gene expression analysis with the Neuroinflammation gene panel (nanoString nCounter), are shown in Fig. 3A ($n = 4$/group) which had been stained with antibodies specific for the neuronal marker NeuN (red color) and an anti-Aβ42 antibody (McSA1, brown color). Not shown are the brain sections from the age and gender matched wild-type controls used throughout the experiments. The 40 μm thick sections contained many different brain regions including all areas of the hippocampus (subiculum, CA1, CA2, CA3, Dentate), midbrain, cortex and cerebellum and thus RNA from all these regions was analyzed in the assay. In 3B, the >50% reduction of amyloid plaques in mice which had received DNA Aβ42 immunizations is illustrated in the enlarged pictures of the subiculum area from the same mouse sections shown in 3A in grey color shades for better visualization of the dark plaque areas. ImageJ was used for the semiquantitative analysis of the reduction in plaque area found in these brains. This result is shown to the right hand side of the graph. A significant reduction was found for the DNA immunized 3xTg-AD mice (blue bar) compared to the non-immunized 3xTg-AD controls (black bar, Wilcoxon exact 2-sided p value 0.029), Reduction of tau was tested in lysates from the same brains shown here

in a Western Blot. Total tau was detected with the moab Tau12 and was significantly reduced in the DNA immunized mice compared to the non-treated 3xTg-AD controls (Wilcoxon exact 2-sided *p* value 0.029, Suppl. Fig. 2).

A multitude of differentially expressed genes were found. Significant changes in transcript levels between non-immunized AD mice and wild-type controls were detected for genes involved in microglia (*Trem2, Ccl3, Csf1, Cd68, Cd84, Apoe, Itgax, Irf8, Ctse, Ctss,* all *p* values <0.05 Kruskal-Wallis test) and astrocyte function (*Cd14, Cd109, Vim, S100a10,* all *p* values <0.05 Kruskal-Wallis test), cytokine and inflammatory signaling (*Mpeg1, Btk, Spp1, Il1r1, Il6ra, Inpp5d, Ch25h, Lilrb4a, Syk, Tgfb1,* all *p* values <0.05 Kruskal-Wallis test), matrix remodeling (*Ptprc, Spp1, Mmp12, Tgfb1,* all *p* values <0.05 Kruskal-Wallis test), apoptosis (*Bcl2a1a, Bax, Casp4*, *Casp8, Fas,* all *p* values <0.05 Kruskal-Wallis test), the innate (*C1qa, C1qb, C1qc, C3ar1, C4a, Btk, Tyrobp, Ly6a, Syk,* all *p* values <0.05 Kruskal-Wallis test) and adaptive immune response (*Cd74, Btk, Ctse, Ctss, Fcer1g, Fcgr2b, Inpp5d, Lilrb4a,* all *p* values <0.05 Kruskal-Wallis test), consistent with an inflammatory phenotype in AD. Examples for these changes in transcript levels of microglia, astrocyte, and cytokine genes are shown in Fig. 4, A–C. From the 700 genes tested in the nanoString Neuroinflammation panel, 139 genes had a ratio difference (fold increase) between wild-type controls and non-treated 3xTg-AD mice greater than 1.4. Most of the genes were upregulated in the transgenic mice in comparison to wild-type mice. From these 139 genes, 50 had ratio differences greater than two; 41 of these genes were also changed in the DNA Aβ42 immunized 3xTg-AD mice compared to the non-immunized AD mice moving into direction of the wild-type controls indicative of downregulation of inflammation due to immunotherapy, respectively (Fig. 4, Table 1). From the 50 genes with a 2-fold ratio difference ($p < 0.05$), 24 genes were genes with microglial function, 11 had astrocyte functions, and 14 genes were involved in inflammatory signaling events, confirming the increase of inflammatory immune reactions and substantial overlap of cellular pathways in late stage AD in the 24 months old 3xTg-AD mouse model.

Considering the material from wild-type mice as far away from amyloid plaques as they have no plaques, and the material from non-immunized 3xTg-AD mice as close to amyloid plaques as they possess high numbers of amyloid plaques in the respective brain sections, significantly high levels of expression were found for the genes involved in microglia function and autophagy, *Cd68, Clec7a, Trem2*, and *Tyrobp* (Fig. 4D). These genes were specifically pointed out as plaque associated genes in sections isolated from brain sections close to and away from amyloid plaques with a laser capture system as highly significant in a customized gene panel (nanoString nCounter, Rothman et al., 2018). Comparison of transcript levels in wild-type mouse brain and non-treated 3xTg-AD mouse brains showed significant differences for *Cd68* ($p = 0.0231$ Kruskal-Wallis), *Clec7a* ($p = 0.0231$), *Trem2* ($p = 0.0244$), and *Tyrobp* ($p = 0.0249$). A lower expression of all four genes was found in the DNA Aβ42 immunized mice compared to the non-immunized 3xTg-AD mice, consistent with removal of amyloid plaques and downregulation of inflammation (Fig. 4D).

Another pair of genes, *Cst7* and *Itgax*, which had recently been identified to be highly expressed in the entorhinal cortex of J20 mice (amyloid AD mouse model) and rTg4510 (tau AD mouse model) and strongly associated with the progression of both pathologies

(Castanho et al., 2020), was also significantly increased in brain samples from the non-immunized group of 3xTg-AD mice compared to the wild-type controls (p values of 0.0057 and 0.0023, Kruskal-Wallis), and reduced in brains of mice which had received DNA Aβ42 immunotherapy (Fig. 4E).

3.6. DNA Aβ42 immunotherapy restored expression of immediate early genes in brain of the 3xTg-AD mouse to levels found in wild-type mouse brains

Significant changes were found for the immediate-early-genes, *Bdnf, Homer1, Egr1,* and *Arc/Arg3*.1 (Fig. 5A) involved in neuronal and neurotransmission pathways and memory formation (Hendrickx et al., 2014; Minatohara et al., 2016; Shepherd and Bear, 2011; Tyssowski et al., 2018) which were significantly higher expressed in DNA Aβ42 immunized 3xTg-AD mice compared to non-immunized 3xTg-AD mice (p values of 0.0243, 0.0331, 0.0427, and 0.0324 Kruskal-Wallis with Dunn's post hoc multiple comparisons test, respectively), indicating effects of DNA Aβ42 immunotherapy on synapse stability and plasticity. BDNF levels were also tested in lysates prepared from the frozen hemibrains (left side) of the same mouse brains used for the nanoString assay and confirmed the results with significantly higher levels in the DNA Aβ42 immunized 3xTg-AD mice compared to the non-immunized mice (Fig. 5B). DNA Aβ42 immunized mice had BDNF levels of 1682 ± 59.5 pg/ml (median ± SIQR) in the respective brain lysates, non-immunized 3xTg-AD had 1155 ± 124.5 pg/ml, and wild-type mice had BDNF levels of 1305 ± 139.5 pg/ml. The p value for the comparison of protein levels between immunized and control 3xTg-AD mice was highly significant ($p = 0.0012$, Kruskal-Wallis with Dunn's post hoc multiple comparisons test). Analysis of the transcript ratios of the IEGs in the 3 groups of mice and graphing of the data in a log2 transformation further illustrated the significance of these results (Fig. 5C and D).

Changes in transcript levels for two other immediate early genes were detected in the mouse AD gene panel; gene expression for *Neuropentraxin 2* (*Ntpx2* or *Narp*) and the secreted nerve growth factor polypeptide *Vgf* (non-acronymic). *Ntpx2* was up in the RNA samples from DNA Aβ42 immunized 3xTg-AD mouse brains with 152 ± 24.95 (median ± SIQR) transcripts compared to the non-treated 3xTg-AD samples (114.1 ± 5.3 transcripts, and similar to the transcript numbers found in the wild-type mouse brain samples (142.9 ± 35.45 transcripts, Fig. 5A). *Vgf* transcripts were significantly increased in brain of DNA Aβ42 immunized 3xTg-AD mice with 511.6 ± 61.85 (median ± semi-interquartile range) copies compared to 414.1 ± 31.65 copies in the non-immunized 3xTg-AD mice (p value 0.0403, Kruskal-Wallis). Wild-type mouse brains had levels of 471.0 ± 67.85 copies for this gene (Fig. 5). *Vgf* has been described as an activity induced gene which is closely linked to *Bdnf* expression with peak levels 3 h after Bdnf incubation in neuronal cell cultures (Alder et al., 2003; Hunsberger et al., 2007).

3.7. DNA Aβ42 immunotherapy restored expression of the circadian clock gene Per1 to wild-type levels

Transcript levels for the *Per1* gene (period circadian clock 1) were significantly decreased in non-immunized 3xTg-AD mice consistent with high levels of Aβ accumulation in brain. While brains from DNA Aβ42 immunized 3xTg-AD mice had similar levels of *Per1*

transcript as wild-type mouse brains (435.4 ± 31 and 438.2 ± 50.2, median ± SIQR), brains from the non-immunized 3xTg-AD mice had significantly lower transcript numbers of 333.9 ± 36.9 ($p = 0.0145$ Kruskal-Wallis, Fig. 6). Thus, DNA Aβ42 immunotherapy restored expression of this circadian clock gene.

3.8. DNA Aβ42 immunotherapy leads to transcriptome changes in disease associated genes and increased expression of genes involved in vesicle trafficking and neurotransmitter release in brain of the 3xTg-AD mouse

Using the Nanostring nCounter mouse AD gene panel for the analysis of the same batch of RNAs isolated from the FFPE sections 24 months old mouse brains, additional changes in neuronal pathways were identified. From the 101 differently expressed genes out of 770 genes included in the mouse AD gene panel, 58 genes were significantly higher expressed in the transgenic mice while 31 genes were significantly lower expressed. Twenty genes had significant changes similarly in both groups of 3xTg-AD mice, and eight genes showed significantly different levels from the wild-type mouse brain controls only in the DNA Aβ42 immunized mice (all p values <0.05 Kruskal-Wallis test, Table 2). Only a small number of genes ($n = 11$) had ratio thresholds larger than 2: These were: *A2m, C1qa, C1qb, C1qc, Ctss, Cyba, Fcer1g, Fxyd5, Pros1, Trem2, and Tyrobp*.

From the 150 disease associated genes (Logsdon et al., 2019, Preuss et al., 2020, KEGG Pathways Database https://genome.jp/kegg/kegg1. html, Reactome, https://reactome.org/cite, and GeneOntology, http://geneontology.org/docs/go-citation-policy) included in the AD gene panel, only 20 genes showed significant increased or reduced expression levels in the 24 months old 3xTg-AD mouse brains (nine genes are shown in Fig. 7, all 20 are included in Table 2). A reduced expression of the disease associated gene *Ndufa5* (NADH ubiquinone oxidoreductase subunit A5) in the non-immunized 3xTg-AD mice (52.38 ± 2.2 transcripts, median ±) was restored to wild-type level in the DNA Aβ43 immunized 3xTg-AD mice (63.24 ± 11.1 and 63.64 ± 2.64 transcripts, respectively, Fig. 8).

Three of the AD disease associated genes, *App. Mapt*, and *Psen1*, are of mouse type in the gene panel, and are thus not different between wild-type and 3xTg-AD mice as the AD mouse model carries the human transgenes driving disease progression for which expression differences were not detected by assay design (supplementary Fig. 3).

From the 46 genes classified as involved in neurotransmitter release (Mouse AD consortium gene panel, Neuropath annotations, www.nanostring.com) only seven showed significant changes in comparison to the wild-type mouse brain: *Adipor1, Atp2b2, Chrm3, Clic1, Gng12, Slc12a5, Slc39a1* (all p values <0.05 Kruskal-Wallis test, Table 2). From 18 genes classified as involved in transmitter synthesis and storage, four genes *Chrnb2, Dnm1, Stx1b, Stxbp1,* were significantly down regulated in non-immunized 3xTg-AD control mouse brains compared to wild-type mouse brain samples (all p values <0.05 Kruskal-Wallis test, Table 2). *Atp2b2, Atp5j2, Slc8a2, Slc12a5,* and *Ndufa5* were found with higher transcript levels in DNA Aβ42 immunized 3xTg-AD mice and wild-type controls compared to non-immunized 3xTg-AD mice, indicating effects of DNA Aβ42 immunotherapy on synapse function (Fig. 8, Table 2). It is highly likely these changes of genes involved in the neurotransmitter pathway are due to removal of the intraneuronal Aβ1–42 due to DNA

Aβ42 trimer immunotherapy, as it had been shown that in particular intraneuronal Aβ in early stages of the disease is responsible for loss of synaptic functions (Parodi et al., 2010, Saura et al., 2015, Ovsepian et al., 2018, Chakroborty et al., 2019).

3.9. Evidence for gene expression changes in many pathways due to DNA Aβ42 immunotherapy in the 3xTg-AD mouse model

To combine all the expression data and provide a visible readout for the results from the mouse Neuroinflammation and mouse AD gene panels, heat maps from the log2 ratios of selected genes and volcano plots were constructed (shown in Figs. 9 and 10). Most genes with significant expression differences between the 3xTg-AD mice and wild-type controls were found for the microglial gene cluster (shown in 9A), the astrocyte gene cluster (9B) in the neuroinflammation panel, and genes classified as disease associated in the mouse AD gene panel (9C). Gene expression levels in wild-type mice were set as 1 (0 in the log2 transformation) and shown with the blue color. Increased gene expression levels are visible with the yellow color shades. From the 24 selected microglial genes with significant expression increase in the non-immunized 3xTg-AD mice, many genes show a clear trend to have levels more similar to the wild-type mouse brains (visible as more blue). Of note: the heatmaps for the microglial genes shown in the graphical abstract and Figure 9A are not identical because the graphical abstract figure contains all microglial genes with ratios >1.4 (41 genes) while the heatmap in 9A contains only microglial genes with ratios >2 (24 genes). A similar trend is obvious for the 21 selected astrocyte genes (9B). A much less pronounced effect on differences in gene expression levels was seen for the genes in the mouse AD gene panel (9C), which is likely due to the old age of the mouse brains used in the experiments consistent with inflammation as a major player in late stage AD and expression of the AD associated genes earlier in AD pathology (Landel et al., 2014).

The volcano plots show statistical significance (log10 *p* value) versus magnitude of change (log2 fold change). It allows for a visual identification of genes with large ratio changes that are also statistically significant, as these may be the most biologically significant genes (Fig. 10). Three different analyses were shown for expression differences from the Neuroinflammation gene panel: 3 T controls vs 3 T DNA (10A), 3 T DNA vs wt (10B), and 3 T controls vs wt (10C). A list of the Top 20 significant differently expressed genes is also included in the figure. Each set of comparison has a number of genes which are unique for this specific comparison. B and C, in which the 3xTg-AD mouse brains were compared to gene expressions in wild-type mouse brains, have mainly genes involved in microglia function and inflammatory signaling consistent with the upregulation of inflammation in both groups with fine differences, while in the comparison in A, which compared the treated and non-treated 3xTg-AD mouse brains, a large number of genes involved in neuronal pathways (7 of 20) were found and is unique for this set of genes. The five immediate-early genes, *Arc, Egr1, Bdnf, Homer1*, and *cfos*, (ordered by significance) fall under the first 13 of the most significant differently expressed genes with *p* values of 0.0006, 0.0020, 0.0031, 0.0075, and 0.0187 (same order as above) in the two groups of 3xTg-AD mice (see also paragraph above in this manuscript, Fig. 5).

The second most significant differently expressed gene in the comparison of the two 3xTg-AD mouse groups was *Kmt2a* (*p* value 0.001, Fig. 10A), having solid copy levels with over 1000 transcript copies in the mouse brain samples. The gene *Kmt2a* encodes a methyltransferase enzyme that adds H3K4Me3 to histone proteins in the promoter regions of many genes leading to an increased and decreased expression of the associated genes, and the gene is therefore annotated in epigenetic regulation pathways. Samples from DNA Aβ42 immunized 3xTg-AD mice had median levels of 1272 ± 53 (SIQR) transcripts compared to 1143 ± 16.5 transcripts in the non-immunized 3xTg-AD ($p = 0.0286$, Mann-Whitney *U* test). Wild-type mouse brain samples had 1297 ± 79.5 *Kmt2a* transcripts with a *p* value of 0.0286 as well in the comparison to non-immunized 3xTg-AD mice. The comparison of expression between wild-type mice and DNA Aβ42 immunized 3xTg-AD mice was not different ($p = 0.6857$). Kmt2a had been shown to be important for memory consolidation in the hippocampus in *Kmt2a* knock-out mouse models (Kerimoglu et al., 2017).

4. Discussion

Data shown here for the first time highlight the many effects found in the 3xTg-AD mouse model after DNA Aβ42 immunotherapy. The 3xTg-AD mouse carries human genes causing plaque and tangle pathology. Even though there is no tau mutation in humans causing AD, the mutation introduced in this mouse strain causes frontotemporal dementia in human patients. Thus, the model is more complete than other mouse models which carry only mutations to accelerate Aβ pathologies and allows more insight into the pathology caused by AD hallmarks, Aβ and tau, and their interaction respectively. We had previously shown that DNA Aβ42 immunotherapy reduced both of these hallmarks in this animal model (Rosenberg et al., 2018), and we show here now clinical benefits such as increased life span and improved behavior in nest building as a daily living activity in the mice which had received active DNA immunotherapy, while Aβ42 peptide immunized mice had the lowest life span. It is highly likely that these findings are related to inflammation found after Aβ42 peptide immunization in mice (Lambracht-Washington et al., 2009, 2011; Rosenberg et al., 2018). Furthermore, we found effects of DNA Aβ42 immunotherapy on gene expression levels on many layers such as synapse function and synaptic stability not only inflammation, and which are highly likely due to the removal of Aβ peptides from brain resulting in changes in local gene expression, which is similar to our previously published findings in which we describe a significantly reduced tau pathology in the brains from 3xTg-AD mice after DNA Aβ42 immunotherapy due to indirect effects such as reduced tau kinase activation due to the removal of Aβ peptides from brain (Rosenberg et al., 2018).

Major impact on disease progression in Alzheimer's disease (AD) derives from inflammation due to innate and adaptive immune responses. DNA Aβ42 trimer immunotherapy in AD mouse models had shown a non-inflammatory immune response and absence of antigen specific T cell proliferation (Lambracht-Washington et al., 2009, 2011; Rosenberg et al., 2018). We also showed the development of a regulatory T cell response in the mouse model which might have an important impact to downregulate potentially inflammatory T cells (Lambracht-Washington and Rosenberg, 2015). As consequence of an adaptive immune response following vaccination, immunological memory is established. This memory is long-lived after infection or vaccination and can be quickly activated

following antigen re-exposure. From results obtained with the very sensitive IFNγ FluoroSpot assay we present in this paper, high level of short lived effector cells as well as long lived effector memory cells in Aβ42 peptide immunized mice while DNA Aβ42 trimer immunized 3xTg-AD mice did not show either short lived effector cells nor long lived effector memory cells which is important for the continuance of a non-inflammatory immune response over time.

The downregulation of inflammatory pathways was further investigated on the level of gene expression in brain tissue. We used the nanoString nCounter® mouse Neuroinflammation gene panel assay, a newly developed system for analyzes of twelve FFPE brain sections in parallel (n = 4 mouse brain sections/group), to test for gene expression differences in non-treated 3xTg-AD mice, DNA Aβ42 immunized 3xTg-AD mice, and wild-type control mice. The majority of the differently expressed genes had higher expression levels in the non-immunized mice compared to the mice which had received DNA Aβ42 immunotherapy which can be interpreted as high levels of inflammatory processes and microglia and astrocyte activation in the non-immunized mice and reduction of inflammation in the DNA Aβ42 immunized mice. From the significant changes in many genes in the non-treated 3xTg-AD mice compared to the age and gender matched wild-type controls, the differences between the two groups of 3xTg-AD mice, treated and non-treated, were not significant with the stringent Kuskal-Wallis statistical test. However, the consistently lower expression of all of the inflammatory genes tested here in the DNA Aβ42 immunized 3xTg-AD mice documents and supports the non-inflammatory signature of DNA Aβ42 immunotherapy for AD prevention. Lower levels of transcripts in the DNA immunized mice compared to the non-immunized 3xTg-AD mice were measured for eleven of the microglial genes, *Hcar2, Itgax, Lilrb4a, Mmp12, Tlr2, Trem2*, *Tyrobp, Apoe, Casp8, Cd300f and Itgsf6;* and six of the genes involved in astrocyte activation, *Agt, Hspb1, Osmr, Serpina2n, Serping,* and *Vim,* further supporting a trend of downregulation of inflammation due to removal of amyloid and plaque from brain and gene expression changes thereof.

Comparing co-expression of inflammatory genes, significantly high levels of expression differences between aged wild-type mice and 3xTg-AD mice was found for four genes involved in microglia function and autophagy, *Cd68, Clec7a, Trem2,* and *Tyrobp*. These genes were specifically pointed out as plaque associated genes in sections isolated from brain sections with a laser capture system as highly significant (Rothman et al., 2018). We found lower expression levels for these four genes as well in the DNA Aβ42 immunized mice compared to the non-immunized 3xTg-AD mice, consistent with removal of amyloid plaques and thus downregulation of inflammation.

Both microglial genes, *Trem2* (Triggering receptor expressed on myeloid cells 2) and *Apoe* (Apolipoprotein E), were upregulated in the non-treated 3xTg-AD mice and lower expressed in the DNA Aβ42 immunized 3xTg-AD mice. Activation of the Trem2-Apoe pathway has been described as leading to loss of the ability of microglia to regulate brain homeostasis. Apoe is a regulator in microglia with disease-associated phenotype and this neurodegenerative phenotype is triggered by Trem2, leasing to consequent activation of Apoe signaling and suppression of the healthy homeostatic microglial phenotype (Krasemann et al., 2017). Similarly, common variants in the gene coding for the membrane-

spanning 4-domains subfamily A (MS4A) protein as an AD risk gene show association with CSF soluble TREM2 concentrations suggestive of modulation of sTREM2 by MS4A (Deming et al., 2019). *Ms4a4* transcript levels were also increased in the non-treated 3xTg-AD mice.

The gene Immunoglobulin superfamily member 6 (*Itgsf6*) was identified as marker gene in a study of microglial genes in aging and neurodegeneration (Bonham et al. 2019). The authors found increased expression of *ITGSF6*, together with *C1QB, C3, CD84*, *FCR1G, LAPTM5, SYK*, and *TLR7* (all genes we also found highly expressed in the 3xTg-AD mouse brain compared to wild-type controls in our gene panel), in specific regions of AD brain (superior temporal gyrus, frontal pole, dorsolateral cortex and parahippocampal gyrus) compared to normal control brain. The brain regions with atrophy early in AD (e.g., superior temporal gyrus and parahippocampal gyrus) were also regions with the highest expression of microglial genes (Bonham et al. 2019). In the mouse brains studied here, we found a significant increase of *Itgsf6* transcripts in the non-immunized 3xTg-AD mice compared to the wild-type brains ($p = 0.0324$, Kruskal-Wallis), and a reduction in the DNA Aβ42 immunized 3xTg-AD mice compared to the non-immunized 3xTg-AD mice which can be interpreted as less neurodegeneration in mice which have received DNA immunotherapy.

To seek for additional gene expression differences in brain in these very old mice, the same RNA samples were used in another assay, the AD mouse gene panel. From the 101 differently expressed genes out of 773 genes included in the mouse AD gene panel, 58 genes were significantly higher expressed in the transgenic mice while 31 genes were significantly lower expressed. Eight genes were elevated or lower expressed in the DNA Aβ42 immunized mice only in the comparison to expression levels in wild-type mouse brain controls (Table 2). This diverse pattern is due to the different gene sets tested for in the two assays: inflammatory genes are generally higher expressed with disease progression (most of the genes tested in the Neuroinflammation panel) while other genes having neuron specific functions like synapse stability and neurotransmitter vesicle release and vesicle recycling are lower expressed with disease progression (many genes in the mouse AD gene panel).

In the comparison of ratio thresholds between the 3xTg-AD mice and wild-type mice, overall much lower ratios for the transcript number differences than in the inflammation gene panel were observed. Only a total of 11 genes had a ratio threshold larger than two: *A2m, C1qa, C1qb, C1qc, Ctss, Cyba, Fcer1g, Fxyd5, Pros1, Trem2, and Tyrobp*. Nine of these were involved in inflammatory immune processes: *C1qa, C1qb, C1qc, Ctss, Cyba, Fcer1g, Fxyd5, Trem2, and Tyrobp. S*even of these were overlapping with the genes found in the Neuroinflammation panel (tested in both panels). *A2m* is classified as a disease associated gene, and also *Pros1* had been described as a potential biomarker for AD (Kim et al., 2019).

From the total number of 150 disease associated genes included in the AD gene panel, only for 22 genes (*A2m, Apoe, Arpc1b, Cldn11, Cldn5, Fn1, Grn, Laptm5, S100a11, Tnfsrf1a, Cd74, Serpinb1a, Stxbp1, B2m, Dmn1, Plp1, Slc39a1, Tgfbr1, Trem2, Tyrobp, Zfp36, Yap,* Table 2) significant increased or reduced expression levels were found in the 24 months old 3xTg-AD mouse brains in comparison to the age and gender matched wild-type mouse

brains. In the comparison to the large number of genes with significant changes in the parallel analyzed Neuroinflammation panel, in which 53 genes had 2-fold expression differences compared to only 11 in the mouse AD panel, these data confirm findings by others that AD associated genes are expressed early in disease progression while inflammation is a late gene signature (Manavalan et al., 2013; Gatta et al., 2014; Landel et al., 2014; Castillo et al., 2017; Castanho et al., 2020). While we do not have the direct comparison of early and late disease in our experiments (young and old mice), results presented here by comparing the number of genes upregulated with the two gene panels confirm that clearly a higher number of genes were upregulated in the Neuroinflammation panel compared to the mouse AD gene panel (Tables 1 and 2). Thus, neuroinflammation is more pronounced in these old mice (late stage disease). Also different from the Neuroinflammation panel in which the genes were in general found to be higher expressed in the non-immunized mice and lower expressed in the mice which had received DNA Aβ42 immunotherapy, a more diverse pattern of gene expression was found for the mouse AD gene panel. This is likely due to the gene sets included in this panel: which contain for example genes involved in neural connectivity, tissue integrity, axon and dendrite structures, and vesicle trafficking.

Synaptic genes are downregulated in AD with disease progression leading to malfunction of synaptic vesicle processing which was found in both groups of 3xTg-AD mice with lower expression for example of the gene *Dynamin 1* (*Dmn1*) compared to wild-type mouse brains, while transcript levels of other genes like *Atp2b2, Atp5j2, Slc12a5, Stx1b, Tbc1d30,* and *Ndufa5* also involved in synaptic vesicle processing are down in the non-immunized 3xTg-AD mice and much higher expressed or even restored to wild-type levels in the DNA Aβ42 immunized 3xTg-AD mouse brains. While an exact mechanism for this result is not known, we would interpret these findings in particular as beneficial effect on brain health in general due to less pathology in the mice which had received DNA anti-Aβ immunotherapy. Genes important for maintenance of circadian rhythms are altered and play a role in AD disease progression as disturbances in the sleep–wake cycle are common symptoms of AD (Musiek et al., 2015). In mouse models it has been shown that an altered sleep cycle reduced Aβ clearance from brain and for the 3xTg-AD mouse model it has been shown that with progression of pathology, clock gene expressions changed in specific brain regions and also according to the light and dark cycles (Kress et al., 2018, Bellanti et al., 2017). In mice which had received DNA Aβ42 immunotherapy, expression of the circadian clock gene *Per1* was significantly increased and restored to wild-type levels in the immunized 3xTg-AD mice.

In both panels, the mouse neuroinflammation and the mouse AD panel, significant increased transcript levels (ratios >2) were found for the *C1q* genes. Binding of C1q is the first component of the classical complement activation pathway leading to cell lysis as defense response in the innate immune system. Fibrillary Aβ and neurofibrillary tau tangles have both been shown to be able to activate the classical complement pathway in vitro in the absence of antibody, which is the normal trigger for the classical complement cascade (Rogers et al., 1998; Chen et al., 1996). Since mouse Aβ differs from human Aβ by three amino acids in the N-terminal region and mouse C1q lacks two of the positively charged residues in the α-chain site critical for optimal Aβ/C1q binding, it was suggested that in

transgenic AD mouse models expressing human Aβ but do not express human C1q, this particular pathway of complement activation is compromised (Akiyama et al., 2000; Webster et al., 1999; Rogers et al., 1998; Chen et al., 1996; Jiang et al., 1994). Data presented here, indicate that beside these possible limitations, *C1q* is highly expressed in 3xTg-AD brain tissue with much lower transcript levels in the DNA Aβ42 immunized 3xTg-AD mice which is likely due to reduction of both complement activators, Aβ and tau (Rosenberg et al., 2018).

Of the 36 genes identified as Plaque-induced-genes (PIGs) which had no overlap with Aβ induced expression of microglial or astrocyte genes (Chen et al., 2020), 21 genes were included in either the mouse neuroinflammation or mouse AD gene panel tested here. Except for *Gns, Igfbp5*, and *Lgmn*, all of these were also significantly increased ($p < 0.05$, non-parametric Kruskal Wallis) in the non-treated 3xTg-AD mouse model compared to the age and gender-matched wild-type controls. *Csf1r* and *Ofml3* were significantly higher in both groups of 3xTg-AD mice (treated and non-treated) with no difference in the transcript numbers, while the remaining 16 PIGs were consistently expressed at lower levels in the DNA Aβ42 immunized mice in accordance with the assumption that amyloid plaques are involved in local gene expression pattern in the brain. In Chen et al., 2020, the authors conclude that further work is needed to show which effects on PIG expression will be seen after removal of amyloid due to immunotherapy. Variations in the outcome of passive immunization in clinical trials can be attributed to the different antibody clones (Gallardo and Holtzman, 2017, Schneider, 2020), as well as to differences comparing active immunization regimen, which we have done by comparing active DNA Aβ42 immunization to active Aβ42 peptide immunization in mouse models (Lambracht-Washington et al., 2009; Rosenberg et al., 2018). To our knowledge, this is the first report showing the effect of DNA Aβ42 immunotherapy on the reduced expression of many genes upregulated in AD brain.

Most importantly, gene expression differences were found in the class of immediate early genes involved in memory formation and synaptic plasticity (Hendrickx et al., 2014; Minatohara et al., 2016; Shepherd and Bear, 2011; Tyssowski et al., 2018). These genes were expressed at lower levels in the non-immunized 3xTg-AD mice and not different in wild-type mice and the DNA immunized 3xTg-AD mice indicating that expression of these genes were restored to wild-type levels due to DNA Aβ42 trimer immunotherapy. In the volcano, plot comparing differently expressed genes in non-immunized 3xTg-AD mice and DNA Aβ42 immunized 3xTg-AD mice, large magnitude changes that are also statistically significant move to the top of the graph. In this statistical test, the immediate early genes, *Arc, Egr1, Bdnf, Homer1*, and *cfos*, in this exact order, moved to the top left side of the graph indicating that these genes have highly significant differences in gene expression between the two groups with low expression in the non-immunized 3xTg-AD controls. In the opposite comparison, 3xTg-AD DNA vs. 3xTg-AD con, these genes move to the other side (right hand side) of the graph, highlighting the significant upregulation of these genes after DNA Aβ42 immunization (exact mirror image, data not shown).

Presynaptic expression of the immediate early gene *Neuropentraxin 2* (*Nptx2, Narp*) regulates excitatory synapses on parvalbumin interneurons which are dependent on the AMPA receptor subunit GluA4. Soluble Nptx2 protein co-localizes with the AMPA receptor

subunits at excitatory synapses and stabilizes the complex through multimeric binding (Chapman et al., 2020, O'Brien et al., 1999, Xiao et al., 2017). Human studies showed that these parvalbumin interneurons are particularly susceptible to degeneration and are up to 60% decreased in numbers in AD brain (Brady and Mufson, 1997). Protein levels of Nptx2 are reduced in CSF of human AD patients and can be correlated to cognitive performance and hippocampal volume (Xiao et al., 2017).

Arc which had been described as the master regulator of synapse plasticity, is probably the most significant gene of the five immediate early genes, *Arc, Bdnf, cfos, Egr1*, and *Homer2* which were found to be altered in the DNA immunized mice (Bramham et al., 2010, Hendrickx et al., 2014, Minatohara et al., 2016). Bdnf expression was confirmed on the protein level with a Bdnf ELISA assay from the same brain samples used for the nanoString nCounter gene expression assays showing also increased Bdnf protein levels in brain from DNA Aβ42 immunized 3xTg-AD mice compared to the non-treated 3xTg-AD controls. Of note, despite the fact that these genes are described as neuronal activity induced genes, we found the described differences in "non-exercised" mice. We do not know how high levels would have been in mice directly following neuronal stimulation directly after exercise or learning, but we present here significant differences for key genes in synaptic plasticity and memory formation in the AD mouse model by comparing groups of mice which had received DNA Aβ42 immunotherapy to reduce brain amyloid and mice which had not received therapy.

5. Conclusions

We present here for the first time, changes in the expression of a multitude of genes in the brains of mice which had received the DNA Aβ42 vaccine. Data presented show the effect of DNA Aβ42 immunotherapy on the downregulation of many inflammatory genes upregulated in AD brain, and the upregulation of a number of immediate early genes involved in memory and synaptic plasticity to levels found in wild-type mouse brains. The fact, that indeed many genes and pathways were altered strongly supports the note of substantial changes on the cellular environment due to the immunotherapy. The consistent finding of inflammatory changes in AD supports future efforts to develop anti-amyloid and anti-inflammatory combination therapies that will strengthen downregulation of inflammatory responses which are in part related to amyloid deposition but also related to independent inflammatory pathways and thus not affected by an anti-amyloid therapy. Data reported here highlight the multitude of changes in the 3xTg-AD mouse model due to DNA Aβ42 immunotherapy only. Furthermore, based on these data, we conclude that active DNA Aβ42 immunotherapy has high potential to be successful in a clinical trial as monotherapy or potentially as a combination therapy in early human AD patients to delay onset of the disease.

Supplementary Material

Refer to Web version on PubMed Central for supplementary material.

Acknowledgements

This work was supported by NIA/NIH P30AG12300–21, NIA/NIH R03AG059201, AWARE, “Triumph Over Alzheimer’s Disease Charity”. The Nanostring Assays were performed at the UTSW Genomics and Microarray core facility. We would like to thank the UTSW Whole Brain Microscopy Facility (WBMF) in the Department of Neurology for assistance with slide scanning. WBMF is supported by the Texas Institute for Brain Injury and Repair (TIBIR).

References

Akiyama H, Barger S, Barnum S, Bradt B, Bauer J, Cole GM, Cooper NR, Eikelenboom P, Emmerling M, Fiebich BL, Finch CE, Frautschy S, Griffin WS, Hampel H, Hull M, Landreth G, Lue L, Mrak R, Mackenzie IR, McGeer PL, O’Banion MK, Pachter J, Pasinetti G, Plata-Salaman C, Rogers J, Rydel R, Shen Y, Streit W, Strohmeyer R, Tooyoma I, Van Muiswinkel FL, Veerhuis R, Walker D, Webster S, Wegrzyniak B, Wenk G, Wyss-Coray T, 2000 Inflammation and Alzheimer’s disease. Neurobiol. Aging 21 (3), 383–421. [PubMed: 10858586]

Alder J, Thakker-Varia S, Bangasser DA, Kuroiwa M, Plummer MR, Shors TJ, Black IB, 2003 Brain-derived neurotrophic factor-induced gene expression reveals novel actions of VGF in hippocampal synaptic plasticity. J. Neurosci 23 (34), 10800–10808. [PubMed: 14645472]

Bellanti F, Iannelli G, Blonda M, Tamborra R, Villani R, Romano A, Calcagnini S, Mazzoccoli G, Vinciguerra M, Gaetani S, Giudetti AM, Vendemiale G, Cassano T, 2017 Serviddio G alterations of clock gene RNA expression in brain regions of a triple transgenic model of Alzheimer’s disease. J. Alzheimers Dis 59 (2), 615–631. [PubMed: 28671110]

Boeddrich A, Babila JT, Wiglenda T, Diez L, Jacob M, Nietfeld W, Huska MR, Haenig C, Groenke N, Buntru A, Blanc E, Vannoni E, Erck C, Friedrich B, Martens H, Neuendorf N, Schnoegl S, Wolfer DP, Loos M, Beule D, Andrade-Navarro MA, Wanker EE, 2019 The Anti-amyloid Compound DO1 Decreases Plaque Pathology and Neuroinflammation-Related Expression Changes in 5xFAD Transgenic Mice. Cell Chem Biol 26 (1), 109–120. [PubMed: 30472115]

Bonham LW, Sirkis DW, Yokoyama JS, 2019 The Transcriptional Landscape of Microglial Genes in Aging and Neurodegenerative Disease. Front Immunol 10, 1170. [PubMed: 31214167]

Brady DR, Mufson EJ, 1997 Parvalbumin-immunoreactive neuronsin the hippocampal formation of Alzheimer’s diseased brain. Neuroscience 80, 1113–1125. [PubMed: 9284064]

Bramham CR, Alme MN, Bittins M, Kuipers SD, Nair RR, Pai B, Panja D, Schubert M, Soule J, Tiron A, Wibrand K, 2010 The arc of synaptic memory. Exp. Brain Res 200 (2), 125–140. [PubMed: 19690847]

Castanho I, Murray TK, Hannon E, Jeffries A, Walker E, Laing E, Baulf H, Harvey J, Bradshaw L, Randall A, Moore K, O’Neill P, Lunnon K, Collier DA, Ahmed Z, O’Neill MJ, Mill J, 2020 Transcriptional signatures of tau and amyloid neuropathology. Cell Rep 30 (6), 2040–2054. [PubMed: 32049030]

Castillo E, Leon J, Mazzei G, Abolhassani N, Haruyama N, Saito T, Saido T, Hokama M, Iwaki T, Ohara T, Ninomiya T, Kiyohara Y, Sakumi K, LaFerla FM, Nakabeppu Y, 2017 Comparative profiling of cortical gene expression in Alzheimer’s disease patients and mouse models demonstrates a link between amyloidosis and neuroinflammation. Sci. Rep 7 (1), 17762. [PubMed: 29259249]

Chakroborty S, Hill ES, Christian DT, Helfrich R, Riley S, Schneider C, Kapecki N, Mustaly-Kalimi S, Seiler FA, Peterson DA, West AR, Vertel BM, Frost WN, Stutzmann GE, 2019 Reduced presynaptic vesicle stores mediate cellular and network plasticity defects in an early-stage mouse model of Alzheimer’s disease. Mol. Neurodegener 14 (1), 7. [PubMed: 30670054]

Chapman G, Shanmugalingam U, Smith PD, 2020 The Role of Neuronal Pentraxin 2 (NP2) in Regulating Glutamatergic Signaling and Neuropathology. Front Cell Neurosci 13, 575. [PubMed: 31969807]

Chen S, Frederickson RC, Brunden KR, 1996 Neuroglial-mediated immunoinflammatory responses in Alzheimer’s disease: complement activation and therapeutic approaches. Neurobiol. Aging 17, 781–787. [PubMed: 8892352]

Chen X, Deane NG, Lewis KB, Li J, Zhu J, Washington MK, Beauchamp RD, 2016 Comparison of Nanostring nCounter® data on FFPE Colon Cancer samples and Affymetrix microarray data on matched frozen tissues. PLoS One 11 (5), e0153784. [PubMed: 27176004]

Chen WT, Lu A, Craessaerts K, Pavie B, Sala Frigerio C, Corthout N, Qian X, Laláková J, Kühnemund M, Voytyuk I, Wolfs L, Mancuso R, Salta E, Balusu S, Snellinx A, Munck S, Jurek A, Fernandez Navarro J, Saido TC, Huitinga I, Lundeberg J, Fiers M, De Strooper B, 2020 Spatial transcriptomics and in situ sequencing to study Alzheimer's disease. Cell 182 (4), 976–991. [PubMed: 32702314]

Deming Y, Filipello F, Cignarella F, Cantoni C, Hsu S, Mikesell R, Li Z, Del-Aguila JL, Dube U, Farias FG, Bradley J, Budde J, Ibanez L, Fernandez MV, Blennow K, Zetterberg H, Heslegrave A, Johansson PM, Svensson J, Nellgård B, Lleo A, Alcolea D, Clarimon J, Rami L, Molinuevo JL, Suárez-Calvet M, Morenas-Rodríguez E, Kleinberger G, Ewers M, Harari O, Haass C, Brett TJ, Benitez BA, Karch CM, Piccio L, Cruchaga C, 2019 The MS4A gene cluster is a key modulator of soluble TREM2 and Alzheimer's disease risk. Sci Transl Med 11 (505).

Dickey CA, Loring JF, Montgomery J, Gordon MN, Eastman PS, Morgan D, 2003 Selectively reduced expression of synaptic plasticity-related genes in amyloid precursor protein + presenilin-1 transgenic mice. J. Neurosci 23 (12), 5219–5226. [PubMed: 12832546]

Evans CF, Davtyan H, Petrushina I, Hovakimyan A, Davtyan A, Hannaman D, Cribbs DH, Agadjanyan MG, Ghochikyan A, 2014 Epitope-based DNA vaccine for Alzheimer's disease: translational study in macaques. Alzheimers Dement 10 (3), 284–295. [PubMed: 23916838]

Fox NC, Black RS, Gilman S, et al., 2005 Effects of Abeta immunization (AN1792) on MRI measures of cerebral volume in Alzheimer disease. Neurology 64 (9), 1563–1572. [PubMed: 15883317]

Gallardo G, Holtzman DM, 2017 Antibody therapeutics targeting Aβ and tau. Cold Spring Harb Perspect Med 7 (10), a024331. [PubMed: 28062555]

Gatta V, D'Aurora M, Granzotto A, Stuppia L, Sensi SL, 2014 2 13 Early and sustained altered expression of aging-related genes in young 3xTg-AD mice. Cell Death Dis 5, e1054. [PubMed: 24525730]

Gilman S, Koller M, Black RS, Jenkins L, Griffith SG, Fox NC, Eisner L, Kirby L, Rovira MB, Forette F, Orgogozo JM, 2005 AN1792(QS-21)-201 Study Team. Clinical effects of Abeta immunization (AN1792) in patients with AD in an interrupted trial. Neurology 64, 1553–1562. [PubMed: 15883316]

Hardy J, Selkoe DJ, 2002 The amyloid hypothesis of Alzheimer's disease: progress and problems on the road to therapeutics. Science 297 (5580), 353–356. [PubMed: 12130773]

Hendrickx A, Pierrot N, Tasiaux B, Schakman O, Kienlen-Campard P, De Smet C, Octave JN, 2014 Epigenetic regulations of immediate early genes expression involved in memory formation by the amyloid precursor protein of Alzheimer disease. PLoS One 9 (6), e99467. [PubMed: 24919190]

Hull M, Sadowsky C, Arai H, Le Prince Leterme G., Holstein A, Booth K, Peng Y, Yoshiyama T, Suzuki H, Ketter N, Liu E, Ryan JM, 2017 Long-term extensions of randomized vaccination trials of ACC-001 and QS-21 in mild to moderate Alzheimer's disease. Curr. Alzheimer Res 14 (7), 696–708. [PubMed: 28124589]

Hunsberger JG, Newton SS, Bennett AH, Duman CH, Russell DS, Salton SR, Duman RS, 2007 Antidepressant actions of the exercise-regulated gene VGF. Nat. Med 13 (12), 1476–1482. [PubMed: 18059283]

Jiang H, Burdick D, Glabe CG, Cotman CW, Tenner AJ, 1994 β -amyloid activates complement by binding to a specific region of the collagen-like domain of the C1q a chain. J. Immunol 152, 5050–5059. [PubMed: 8176223]

Karran E, De Strooper B, 2016 The amyloid cascade hypothesis: are we poised for success or failure? J. Neurochem 139 (Suppl. 2), 237–252. [PubMed: 27255958]

Kerimoglu C, Sakib MS, Jain G, Benito E, Burkhardt S, Capece V, Kaurani L, Halder R, Agís-Balboa RC, Stilling R, Urbanke H, Kranz A, Stewart AF, Fischer A, 2017 KMT2A and KMT2B mediate memory function by affecting distinct genomic regions. Cell Rep 20 (3), 538–548. [PubMed: 28723559]

Kilkenny C, Browne WJ, Cuthill IC, Emerson M, Altman DG, 2010 Improving bioscience research reporting: the ARRIVE guidelines for reporting animal research. PLoS Biol 8 (6), e1000412. [PubMed: 20613859]

Kim DK, Han D, Park J, Choi H, Park JC, Cha MY, Woo J, Byun MS, Lee DY, Kim Y, Mook-Jung I, 2019 Deep proteome profiling of the hippocampus in the 5xFAD mouse model reveals biological process alterations and a novel biomarker of Alzheimer's disease. Exp Mol Med 51 (11), 1–17.

Krasemann S, Madore C, Cialic R, Baufeld C, Calcagno N, El Fatimy R, Beckers L, O'Loughlin E, Xu Y, Fanek Z, Greco DJ, Smith ST, Tweet G, Humulock Z, Zrzavy T, Conde-Sanroman P, Gacias M, Weng Z, Chen H, Tjon E, Mazaheri F, Hartmann K, Madi A, Ulrich JD, Glatzel M, Worthmann A, Heeren J, Budnik B, Lemere C, Ikezu T, Heppner FL, Litvak V, Holtzman DM, Lassmann H, Weiner HL, Ochando J, Haass C, Butovsky O, 2017 The TREM2-APOE pathway drives the transcriptional phenotype of dysfunctional microglia in neurodegenerative diseases. Immunity 47 (3), 566–581. [PubMed: 28930663]

Kress GJ, Liao F, Dimitry J, Cedeno MR, FitzGerald GA, Holtzman DM, Musiek ES, 2018 Regulation of amyloid-β dynamics and pathology by the circadian clock. J. Exp. Med 215 (4), 1059–1068. 4 2. [PubMed: 29382695]

Lambracht-Washington D, Rosenberg RN, 2015 Co-stimulation with TNF receptor superfamily 4/25 antibodies enhances in-vivo expansion of CD4+CD25+Foxp3+ T cells (Tregs) in a mouse study for active DNA Aβ42 immunotherapy. J. Neuroimmunol 278, 90–99. [PubMed: 25595257]

Lambracht-Washington D, Qu BX, Fu M, Eagar TN, Stüve O, Rosenberg RN, 2009 DNA beta-amyloid (1–42) trimer immunization for Alzheimer disease in a wild-type mouse model. JAMA 302 (16), 1796–1802. [PubMed: 19861672]

Lambracht-Washington D, Qu BX, Fu M, Anderson LD Jr., Stüve O, Eagar TN, Rosenberg RN, 2011 DNA immunization against amyloid beta 42 has high potential as safe therapy for Alzheimer's disease as it diminishes antigen-specific Th1 and Th17 cell proliferation. Cell. Mol. Neurobiol 31, 867–874. [PubMed: 21625960]

Landel V, Baranger K, Virard I, Loriod B, Khrestchatisky M, Rivera S, Benech P, Féron F, 2014 Temporal gene profiling of the 5xFAD transgenic mouse model highlights the importance of microglial activation in Alzheimer's disease. Mol. Neurodegener 9, 33. [PubMed: 25213090]

Li W, Freudenberg J, Suh YJ, Yang Y, 2014 Using volcano plots and regularized-chi statistics in genetic association studies. Comput. Biol. Chem 48, 77–83. [PubMed: 23602812]

Logsdon BA, Perumal TM, Swarup V, Wang M, Funk C, Gaiteri C, Allen M, Wang X, Dammer E, Srivastava G, Mukherjee S, Sieberts SK, Omberg L, Dang KD, Eddy JA, Snyder P, Chae Y, Amberkar S, Wei W, Hide W, Preuss C, Ergun A, Ebert PJ, Airey DC, Carter GW, Mostafavi S, Yu L, Klein H-U, the AMP-AD Consortium, Collier DA, Golde T, Levey A, Bennett DA, Estrada K, Decker M, Liu Z, Shulman JM, Zhang B, Schadt E, De Jager PL, Price ND, Ertekin-Taner N, Mangravite LM, 2019 Meta-analysis of the human brain transcriptome identifies heterogeneity across human AD coexpression modules robust to sample collection and methodological approach. bioRxiv 510420 10.1101/510420.

Makin S, 2018 The amyloid hypothesis on trial. Nature 559 (7715), S4–S7. [PubMed: 30046080]

Manavalan A, Mishra M, Feng L, Sze SK, Akatsu H, Heese K, 2013 9 6 Brain site-specific proteome changes in aging-related dementia. Exp. Mol. Med 45, e39. [PubMed: 24008896]

Matsumoto Y, Niimi N, Kohyama K, 2013 Development of a new DNA vaccine for Alzheimer disease targeting a wide range of aβ species and amyloidogenic peptides. PLoS One 8 (9), e75203. [PubMed: 24086465]

Minatohara K, Akiyoshi M, Okuno H, 2016 Role of immediate-early genes in synaptic plasticity and neuronal ensembles underlying the memory trace. Front. Mol. Neurosci 8, 78. [PubMed: 26778955]

Musiek ES, Xiong DD, Holtzman DM, 2015 Sleep, circadian rhythms, and the pathogenesis of Alzheimer disease. Exp. Mol. Med 47, e148. [PubMed: 25766617]

Naj AC, Jun G, Reitz C, Kunkle BW, Perry W, Park YS, Beecham GW, Rajbhandary RA, Hamilton-Nelson KL, Wang LS, Kauwe JS, Huentelman MJ, Myers AJ, Bird TD, Boeve BF, Baldwin CT, Jarvik GP, Crane PK, Rogaeva E, Barmada MM, Demirci FY, Cruchaga C, Kramer PL, Ertekin-Taner N, Hardy J, Graff-Radford NR, Green RC, Larson EB, George-Hyslop PH St, Buxbaum JD, Evans DA, Schneider JA, Lunetta KL, Kamboh MI, Saykin AJ, Reiman EM, De Jager PL, Bennett

DA, Morris JC, Montine TJ, Goate AM, Blacker D, Tsuang DW, Hakonarson H, Kukull WA, Foroud TM, Martin ER, Haines JL, Mayeux RP, Farrer LA, Schellenberg GD, Pericak-Vance MA, Alzheimer Disease Genetics Consortium, Albert MS, Albin RL, Apostolova LG, Arnold SE, Barber R, Barnes LL, Beach TG, Becker JT, Beekly D, Bigio EH, Bowen JD, Boxer A, Burke JR, Cairns NJ, Cantwell LB, Cao C, Carlson CS, Carney RM, Carrasquillo MM, Carroll SL, Chui HC, Clark DG, Corneveaux J, Cribbs DH, Crocco EA, De Carli C, DeKosky ST, Dick M, Dickson DW, Duara R, Faber KM, Fallon KB, Farlow MR, Ferris S, Frosch MP, Galasko DR, Ganguli M, Gearing M, Geschwind DH, Ghetti B, Gilbert JR, Glass JD, Growdon JH, Hamilton RL, Harrell LE, Head E, Honig LS, Hulette CM, Hyman BT, Jicha GA, Jin LW, Karydas A, Kaye JA, Kim R, Koo EH, Kowall NW, Kramer JH, LaFerla FM, Lah JJ, Leverenz JB, Levey AI, Li G, Lieberman AP, Lin CF, Lopez OL, Lyketsos CG, Mack WJ, Martiniuk F, Mash DC, Masliah E, McCormick WC, McCurry SM, McDavid AN, McKee AC, Mesulam M, Miller BL, Miller CA, Miller JW, Murrell JR, Olichney JM, Pankratz VS, Parisi JE, Paulson HL, Peskind E, Petersen RC, Pierce A, Poon WW, Potter H, Quinn JF, Raj A, Raskind M, Reisberg B, Ringman JM, Roberson ED, Rosen HJ, Rosenberg RN, Sano M, Schneider LS, Seeley WW, Smith AG, Sonnen JA, Spina S, Stern RA, Tanzi RE, Thornton-Wells TA, Trojanowski JQ, Troncoso JC, Valladares O, Van Deerlin VM, Van Eldik LJ, Vardarajan BN, Vinters HV, Vonsattel JP, Weintraub S, Welsh-Bohmer KA, Williamson J, Wishnek S, Woltjer RL, Wright CB, Younkin SG, Yu CE, Yu L, 2014 Effects of multiple genetic loci on age at onset in late-onset Alzheimer disease: a genome-wide association study. JAMA Neurol 71 (11) (1394–404). [PubMed: 25199842]

O'Brien RJ, Xu D, Petralia RS, Steward O, Huganir RL, Worley P, 1999 Synaptic clustering of AMPA receptors by the extracellular immediate-early gene product Narp. Neuron 23 (2), 309–323. [PubMed: 10399937]

Oddo S, Caccamo A, Shepherd JD, Murphy MP, Golde TE, Kayed R, Metherate R, Mattson MP, Akbari Y, LaFerla FM, 2003 Triple-transgenic model of Alzheimer's disease with plaques and tangles: intracellular Abeta and synaptic dysfunction. Neuron 39 (3), 409–421. [PubMed: 12895417]

Orgogozo JM, Gilman S, Dartigues JF, et al., 2003 Subacute meningoencephalitis in a subset of patients with AD after Abeta42 immunization. Neurology 61 (1), 46–54. [PubMed: 12847155]

Ovsepian SV, O'Leary VB, Zaborszky L, Ntziachristos V, Dolly JO, 2018 Synaptic vesicle cycle and amyloid β: biting the hand that feeds. Alzheimers Dement 14 (4), 502–513. [PubMed: 29494806]

Parodi J, Sepúlveda FJ, Roa J, Opazo C, Inestrosa NC, Aguayo LG, 2010 Beta-amyloid causes depletion of synaptic vesicles leading to neurotransmission failure. J. Biol. Chem. 285 (4), 2506–2514. [PubMed: 19915004]

Pasquier F, Sadowsky C, Holstein A, Leterme Gle P, Peng Y, Jackson N, Fox NC, Ketter N, Liu E, 2016 Ryan JM; ACC-001 (QS-21) study team. Two phase 2 multiple ascending-dose studies of Vanutide Cridificar (ACC-001) and QS-21 adjuvant in mild-to-moderate Alzheimer's disease. J. Alzheimers Dis 51 (4), 1131–1143. [PubMed: 26967206]

Preuss C, Pandey R, Piazzae Fine A., Uyar A, Perumal T, Garceau D, Kotredes KP, Williams H, Mangravite LM, Lamb BT, Oblak AL, Howell GR, Sasner M, Logsdon BA, Carter GW, 2020 A novel systems biology approach to evaluate mouse models of late-onset Alzheimer's disease. bioRxiv 682856 10.1101/682856.

Qu BX, Lambracht-Washington D, Fu M, Eagar TN, Stüve O, Rosenberg RN, 2010 Analysis of three plasmid systems for use in DNA Aβ42 immunization as therapy for Alzheimer's disease. Vaccine 28 (32), 5280–5287. [PubMed: 20562015]

Reis PP, Waldron L, Goswami RS, Xu W, Xuan Y, Perez-Ordonez B, Gullane P, Irish J, Jurisica I, Kamel-Reid S, 2011 mRNA transcript quantification in archival samples using multiplexed, color-coded probes. BMC Biotechnol 11, 46. [PubMed: 21549012]

Rogers J, Lue LF, Yang LB, et al., 1998 Complement activation by neurofibrillary tangles in Alzheimer's disease. Neuroscience 24, 1268 (Abstract).

Rosenberg RN, Lambracht-Washington D, 2020 Active immunotherapy to prevent Alzheimer disease-a DNA amyloid β 1–42 Trimer vaccine. JAMA Neurol 77 (3), 289–290. [PubMed: 31816028]

Rosenberg RN, Lambracht-Washington D, Yu G, Xia W, 2016 Genomics of Alzheimer disease: a review. JAMA Neurol 73 (7), 867. [PubMed: 27135718]

Rosenberg RN, Fu M, Lambracht-Washington D, 2018 Active full-length DNA Aβ42 immunization in 3xTg-AD mice reduces not only amyloid deposition but also tau pathology. Alzheimers Res. Ther 10 (1), 115. [PubMed: 30454039]

Rothman SM, Tanis KQ, Gandhi P, Malkov V, Marcus J, Pearson M, Stevens R, Gilliland J, Ware C, Mahadomrongkul V, O'Loughlin E, Zeballos G, Smith R, Howell BJ, Klappenbach J, Kennedy M, Mirescu C, 2018 Human Alzheimer's disease gene expression signatures and immune profile in APP mouse models: a discrete transcriptomic view of Aβ plaque pathology. J. Neuroinflammation 15 (1), 256. [PubMed: 30189875]

Samaey C, Schreurs A, Stroobants S, Balschun D, 2019 Early cognitive and Behavioral deficits in mouse models for Tauopathy and Alzheimer's disease. Front. Aging Neurosci 11, 335. [PubMed: 31866856]

Saura CA, Parra-Damas A, Enriquez-Barreto L, 2015 Gene expression parallels synaptic excitability and plasticity changes in Alzheimer's disease. Front. Cell. Neurosci 9, 318. [PubMed: 26379494]

Schilling S, Rahfeld JU, Lues I, Lemere CA, 2018 Passive Aβ immunotherapy: current achievements and future perspectives. Molecules 23 (5), 1068.

Schneider L, 2020 A resurrection of aducanumab for Alzheimer's disease. Lancet Neurol 19 (2), 111–112. [PubMed: 31978357]

Selkoe DJ, 2019 Early network dysfunction in Alzheimer's disease. Science 365 (6453), 540–541. [PubMed: 31395769]

Selkoe DJ, Hardy J, 2016 The amyloid hypothesis of Alzheimer's disease at 25 years. EMBO Mol Med 8 (6), 595–608. [PubMed: 27025652]

Shepherd JD, Bear MF, 2011 New views of arc, a master regulator of synaptic plasticity. Nat. Neurosci 14 (3), 279–284. [PubMed: 21278731]

Torres-Lista V, Giménez-Llort L, 2013 Impairment of nesting behaviour in 3xTg-AD mice. Behav. Brain Res 247, 153–157. [PubMed: 23523959]

Tyssowski KM, DeStefino NR, Cho JH, Dunn CJ, Poston RG, Carty CE, Jones RD, Chang SM, Romeo P, Wurzelmann MK, Ward JM, Andermann ML, Saha RN, Dudek SM, Gray JM, 2018 Different neuronal activity patterns induce different gene expression programs. Neuron 98 (3) (530–546.e11). [PubMed: 29681534]

Vandenberghe R, Riviere ME, Caputo A, Sovago J, Maguire RP, Farlow M, Marotta G, Sanchez-Valle R, Scheltens P, Ryan JM, Graf A, 2016 Active Aβ immunotherapy CAD106 in Alzheimer's disease: a phase 2b study. Alzheimers Dement (N Y) 3 (1), 10–22. [PubMed: 29067316]

Waggott D, Chu K, Yin S, Wouters BG, Liu FF, Boutros PC, 2012 NanoStringNorm: an extensible R package for the pre-processing of NanoString mRNA and miRNA data. Bioinformatics 28 (11), 1546–1548. [PubMed: 22513995]

Wang CY, Wang PN, Chiu MJ, Finstad CL, Lin F, Lynn S, Tai YH, De Fang X, Zhao K, Hung CH, Tseng Y, Peng WJ, Wang J, Yu CC, Kuo BS, Frohna PA, 2017 UB-311, a novel UBITh® amyloid β peptide vaccine for mild Alzheimer's disease. Alzheimers Dement (NY) 3 (2), 262–272.

Webster S, Tenner AJ, Poulos TL, Cribbs D, 1999 The mouse C1q a chain sequence alters beta amyloid induced complement activation. Neurobiol. Aging 20, 297–304. [PubMed: 10588577]

Winblad B, Andreasen N, Minthon L, Floesser A, Imbert G, Dumortier T, Maguire RP, Blennow K, Lundmark J, Staufenbiel M, Orgogozo JM, Graf A, 2012 Safety, tolerability, and antibody response of active Aβ immunotherapy with CAD106 in patients with Alzheimer's disease: randomised, double-blind, placebo-controlled, first-in-human study. Lancet Neurol 11 (7), 597–604. [PubMed: 22677258]

Xiao MF, Xu D, Craig MT, Pelkey KA, Chien CC, Shi Y, Zhang J, Resnick S, Pletnikova O, Salmon D, Brewer J, Edland S, Wegiel J, Tycko B, Savonenko A, Reeves RH, Troncoso JC, McBain CJ, Galasko D, Worley PF, 2017 NPTX2 and cognitive dysfunction in Alzheimer's Disease. Elife 6 (pii: e23798). [PubMed: 28440221]

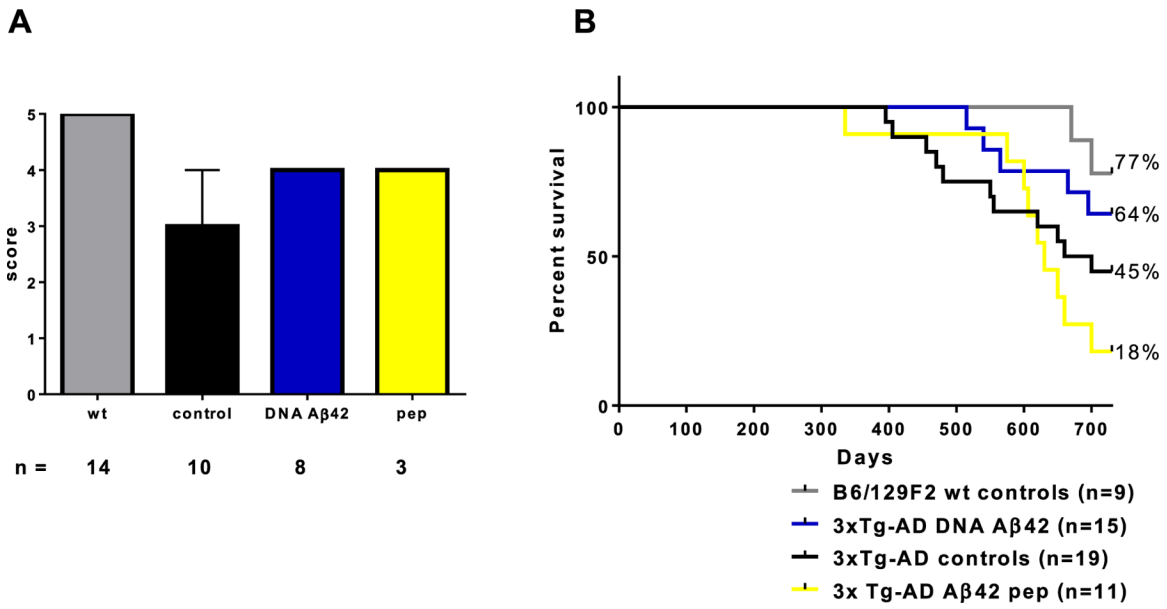

Fig. 1.

Clinical benefits due to DNA Aβ42 immunotherapy in the 3xTg-AD mouse model. A) Natural behavior of nest building: Nesting was assessed in groups of 24 months old 3xTg-AD mice which had received DNA Aβ42 injection via gene gun delivery into the skin (blue bars, $n = 8$) or i.p. Aβ42 peptide injection (yellow bars, $n = 3$), non-immunized 3xTg-AD control mice (black bars, $n = 10$), and age and gender matched B6129F2 wild-type mice were used as healthy control groups (grey bars, $n = 14$). Shown are median values with interquartile change. DNA immunized mice performed better than the not treated 3xTg-AD control mice. Of note: because the wild-type mice did not build significantly better nests than the 3xTg-AD mice, additional 24 months old B6129F2 females were included in this test (total number of mice tested was n = 14). These additional mice were not included in the Life Span analyzes shown in B with nine wild-type mice. B) Increased Life Span in DNA Aβ42 trimer immunized 3xTg-AD mice: Kaplan Meier Survival curve shows 24 months survival in wild-type mice which is illustrated with a grey line, 24 months survival in DNA Aβ42 immunized 3xTg-AD mice which is illustrated with a blue line. Survival curves of Aβ42 peptide immunized and non-immunized 3xTg-AD mice are the yellow and black lines, respectively. Total mouse numbers at the beginning of the experimental time line were shown below the graph in Fig. 1B.

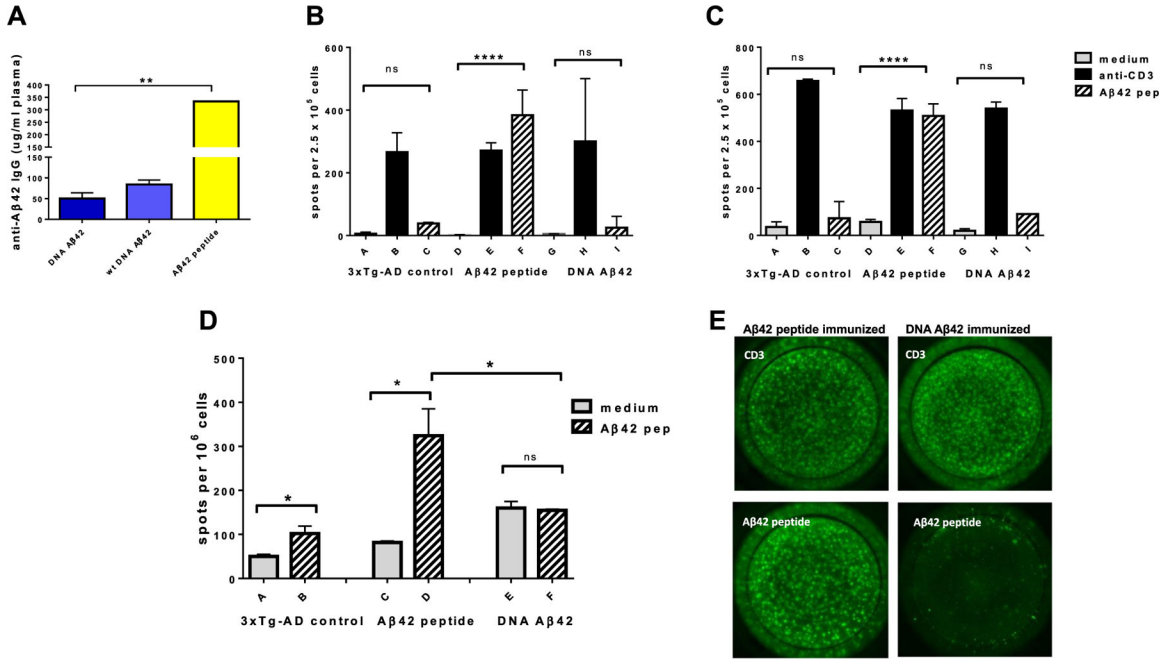

Fig. 2.

Immune responses in mice after anti-amyloid immunotherapy. A) Anti-Aβ42 antibodies in 24 months old mice: Anti-Aβ42 antibody levels in mouse plasma were determined using a standard ELISA assay. Dark blue bars show antibody levels in 24 months old 3xTg-AD mice which had received DNA Aβ42 immunizations (n = 8), light blue bars show antibody levels in DNA Aβ42 immunized B6129F2 wild-type mice (*n* = 5), and yellow bars show antibody levels in Aβ42 peptide immunized 3xTg-AD mice (n = 3). Statistical significance shown in the graph derived from Kruskal-Wallis followed by Dunn's test for statistical comparison of the groups. B and C) No production of inflammatory cytokine in re-stimulated splenocytes from DNA Aβ42 trimer immunized 3xTg-AD mice. IFNγ and IL-17 FluoroSpots in 3xTg-AD control mice (*n* = 4), Aβ42 peptide immunized mice (n = 3) and DNA Aβ42 trimer immunized mice (n = 4). Light grey bars show spot counts in medium control wells, black bars show spot counts in the positive control wells (anti-CD3 moab stimulation), and striped bars show spot counts for Aβ42 peptide re-stimulated splenocytes. Shown are median values with interquartile change. Statistical significance shown in the graph derived from Mann-Whitney statistical comparison of the groups.. D) IFNγ FluoroSpots counted from 3xTg-AD control mice (n = 4), Aβ42 peptide immunized mice (n = 3) and DNA Aβ42 trimer immunized mice (n = 4) in a T cell memory assay. Light grey bars show spot counts for cells which had been cultured in medium with IL-2 for 10 days (control wells), and striped bars show spot counts for cells which had been re-stimulated with Aβ42 peptide and IL-2 for 10 days. Shown are median values with interquartile change. Statistical significance shown in the graph derived from non-parametric Mann-Whitney statistical comparison of the groups. E) Illustrates spot intensity in the IFNγ FluoroSpot; upper panel shows spots in positive control wells (anti-CD3 moab, 48 h) of splenocytes from peptide (left side images) and DNA immunized mice (right side images), lower panel shows spots in wells after Aβ42 peptide re-stimulation for 48 h. Very low spot counts were found in the wells from DNA immunized mice (right image, lower panel).

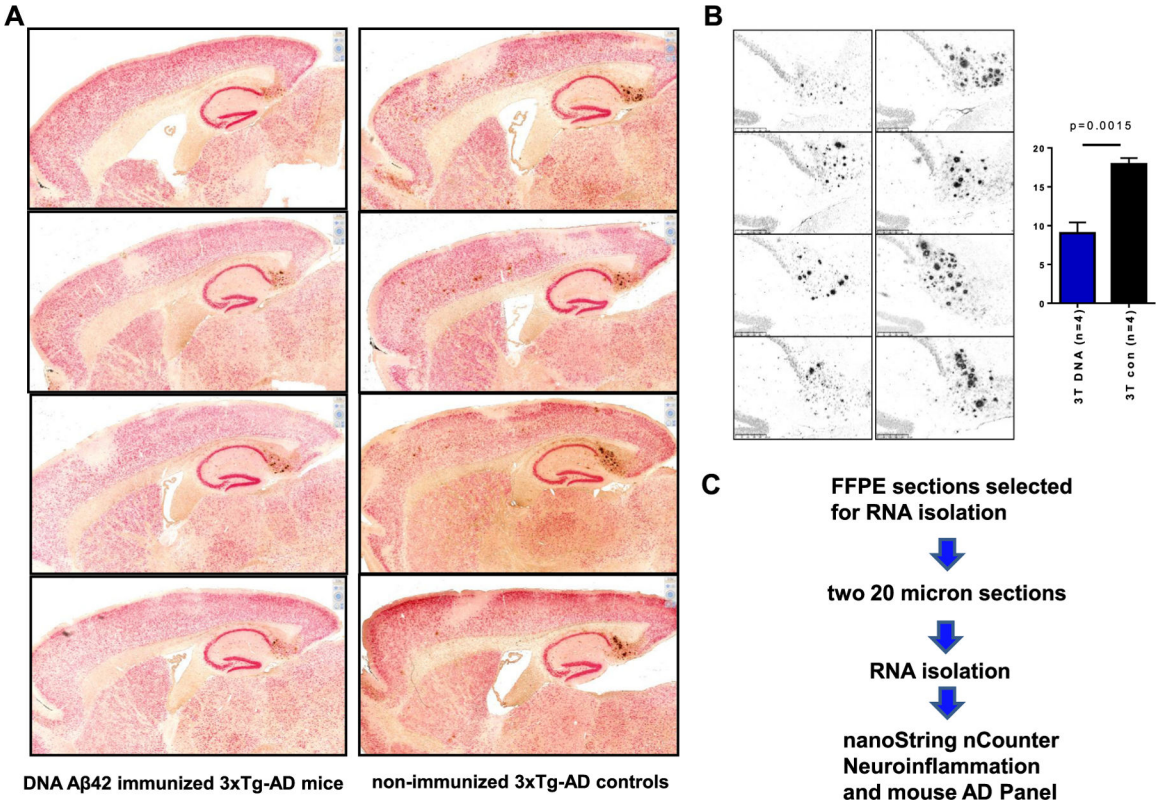

Fig. 3.

Mouse brains selected for the transcriptome analyses. A) Shown are the selected sections (n = 4 for DNA Aβ42 immunized 3xTg-AD female mice. and n = 4 for the non-treated 3xTg-AD female controls) in low magnification to give an overview across the entire sections stained with a NeuN antibody as neuron marker (red color) and an antibody dectecting Aβ1–42 (McSA1, brown color). In B, the subiculum areas of the same sections is enlarged and reduced to grey color shades for better visualization of the dark colored plaque areas present. The four right hand sections were sections from DNA Aβ42 immunized 3xTg-AD mice in the same order as in A; the four left hand sections were from the non-immunized 3xTg-AD controls, respectively. The bar graph to the right hand side illustrated the ImageJ semiquantitative analysis of plaque density in the subiculum of the brain sections shown. The black bar is for the non-immunized 3xTg-AD control mice, the blue bar is for the DNA Aβ42 immunized mice. C) Workflow of the transcriptome analyzes.

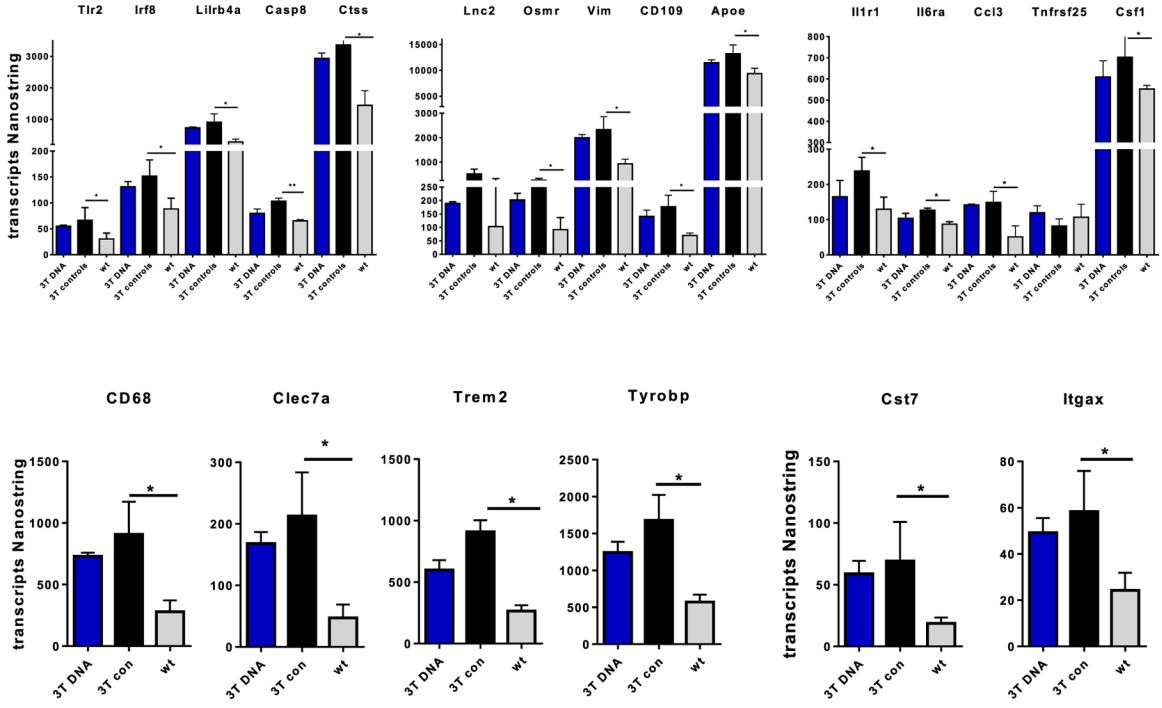

Fig. 4.

Results from the Nanostring Mouse Neuroinflammation gene panel. Changes in gene expression profiles in the comparison of 24 months old DNA Aβ42 immunized 3xTg-AD mice (blue bars, n = 4), 3xTg-AD control mice (black bars, n = 4), and wild-type mice (grey bars, n = 4). A) Shows genes involved in microglia function, B) shows genes important for astrocyte functions, and C) shows genes classified as involved in cytokine signaling pathways. D) Effects of DNA Aβ42 trimer immunization on transcript levels of selected inflammatory genes in brain tissue. Significantly upregulated inflammatory genes in non-immunized 3xTg-AD mice compared to wild-type control mice were down in DNA Aβ42 trimer immunized 3xTg-AD mice. E) Transcript levels for genes *Cst7* and *Itgax*. *, **, indicate *p* values of <0.05 and <0.01 Kruskal-Wallis test. Shown are median values with interquartile change.

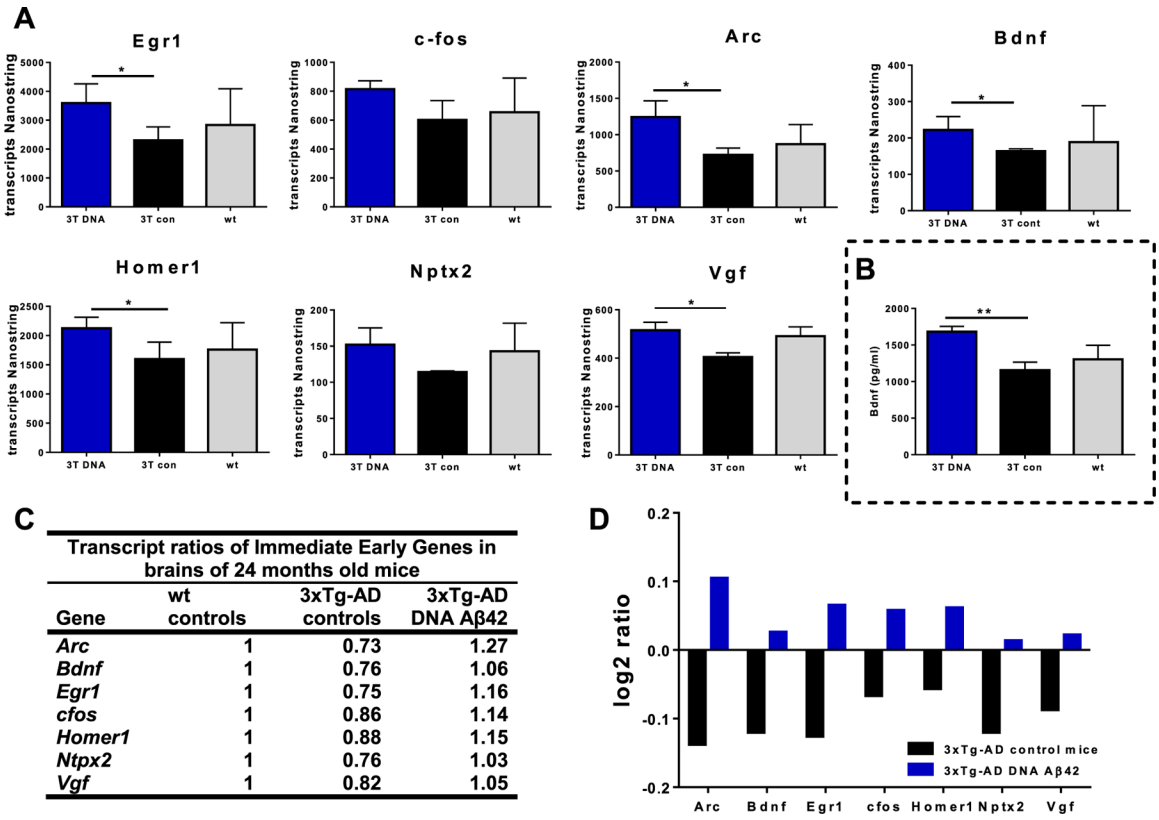

Transcript ratios of Immediate Early Genes in brains of 24 months old mice

Gene	wt controls	3xTg-AD controls	3xTg-AD DNA Aβ42
Arc	1	0.73	1.27
Bdnf	1	0.76	1.06
Egr1	1	0.75	1.16
cfos	1	0.86	1.14
Homer1	1	0.88	1.15
Ntpx2	1	0.76	1.03
Vgf	1	0.82	1.05

Fig. 5.

Transcript numbers of immediate-early- genes in RNA samples from brain sections of 24 month-old mice analyzed with the mouse neuroinflammation and AD gene panels. DNA Aβ42 immunized 3xTg-AD mice are shown in blue bars (n = 4), non-immunized 3xTg-AD controls are shown in black bars (n = 4), and wild-type controls (n = 4) are shown in grey bars. Results shown are representative of two independent assays run using the same RNA samples. A) Shows the transcript numbers for the genes *Egr1, cfos, Homer1*, *Arc*, *Ntpx2, Vgf,* and *Bdnf*. *, ** indicates *p* values of <0.05 and < 0.01, Kruskal-Wallis, shown are median values with interquartile change. B) Shows the results from an ELISA confirming significantly increased Bdnf levels in brains from 24 months old 3xTg-AD mice which had received DNA Aβ42 immunotherapy in comparison to the non-immunized 3xTg-AD controls, *p* value of 0.0012, Kruskal-Wallis, shown are median values with interquartile change. C) Table showing the ratio differences in the three mouse groups, levels in wt mice was set as 1, D) Illustrates the ratio analysis in a log2 transformation graph.

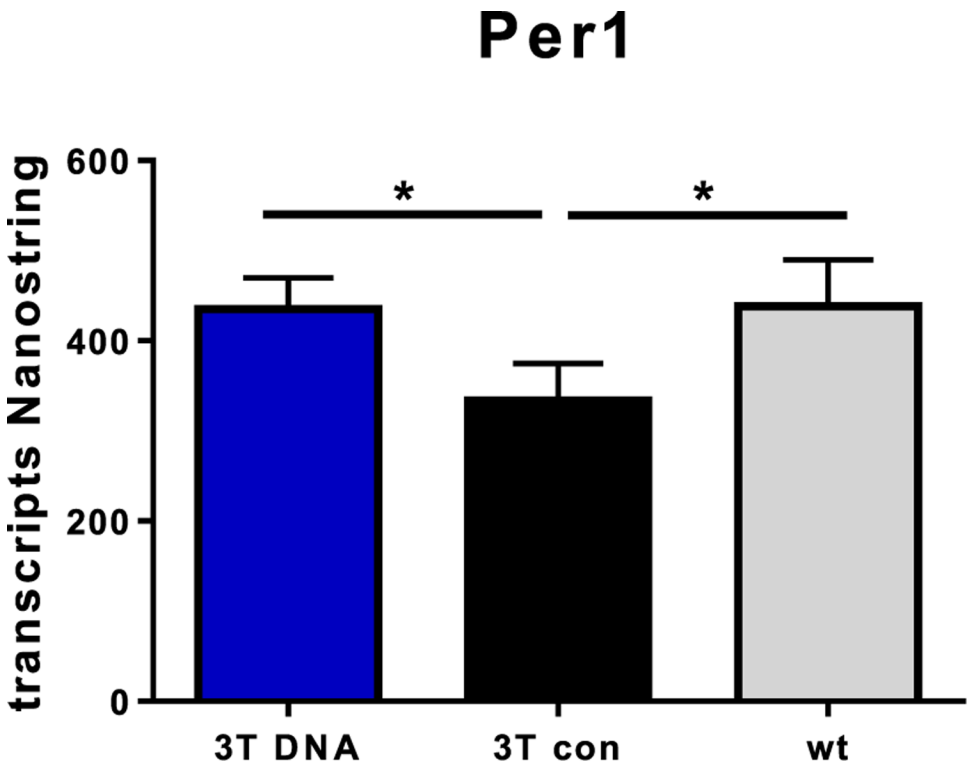

Fig. 6.

DNA Aβ42 immunization restores expression of the Period circadian clock 1 gene (*Per1*) to wild-type levels. Transcript levels from DNA Aβ42 immunized 3xTg-AD mice are shown in blue bars (n = 4), non-immunized 3xTg-AD mice are shown in black bars (n = 4), and age and gender matched wild-type controls are shown in grey bars (n = 4). *p* value of 0.0145 Kruskal-Wallis, shown are median values with interquartile change.

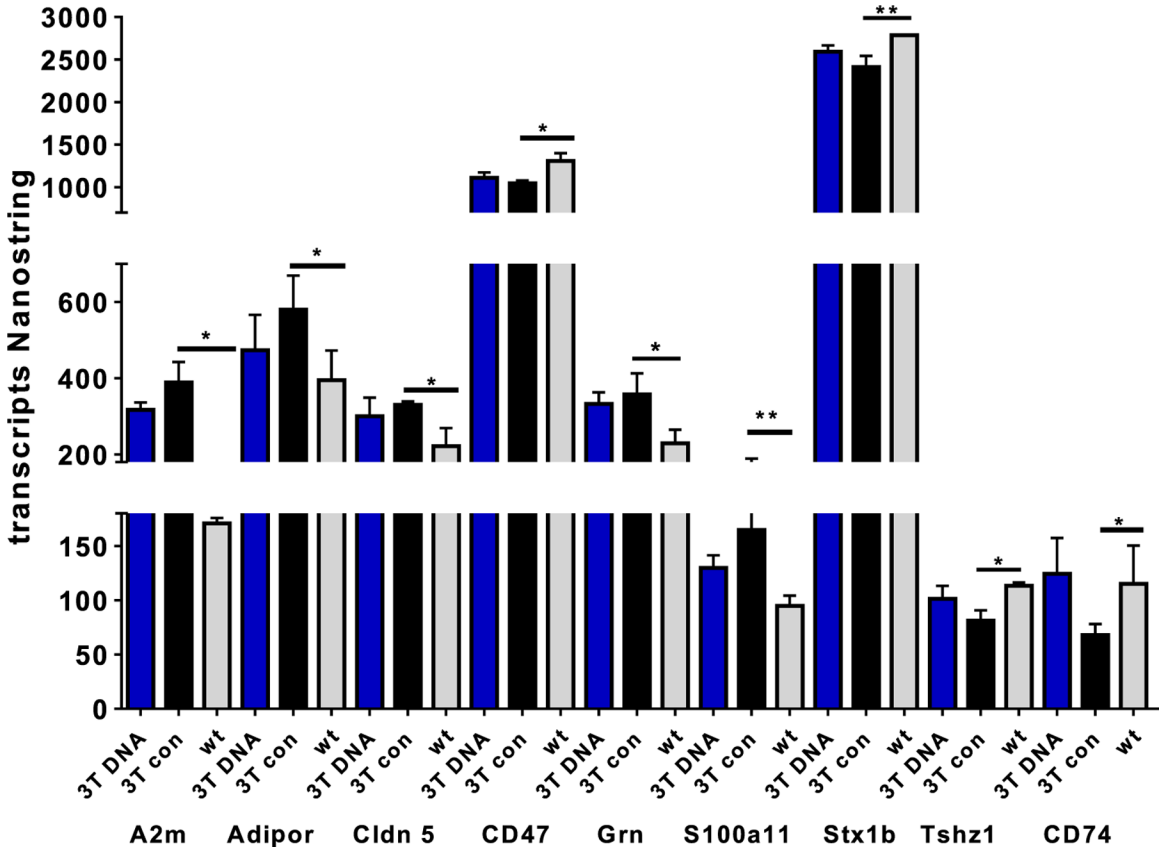

Fig. 7.

Transcript levels of eight disease associated genes analyzed with the mouse AD gene panel. Genes *A2m* (Alpha-2 macroglobulin), *Adipor* (adiponectin receptor 2), *Cldn5* (claudin 5), *Cd47* (CD47 antigen, Rh-related antigen, integrin-associated signal transducer), *Grn* (granulin), *S100a11* (S100 calcium binding protein A11), *Stx1b* (syntaxin 1B), *Tshz1* (teashirt zinc finger family member 1), and *CD74* (CD74 antigen, invariant polypeptide of major histocompatibility complex, class II antigen-associated) showed significant altered transcript levels in the 3xTg-AD mice (blue bars are DNA Aβ42 immunized mice, n = 4, black bars are non-immunized controls, n = 4) compared to the wild-type mouse brain samples (grey bars, n = 4). Shown are the median values with interquartile range, * indicates *p* values of <0.05, Kruskal-Wallis test.

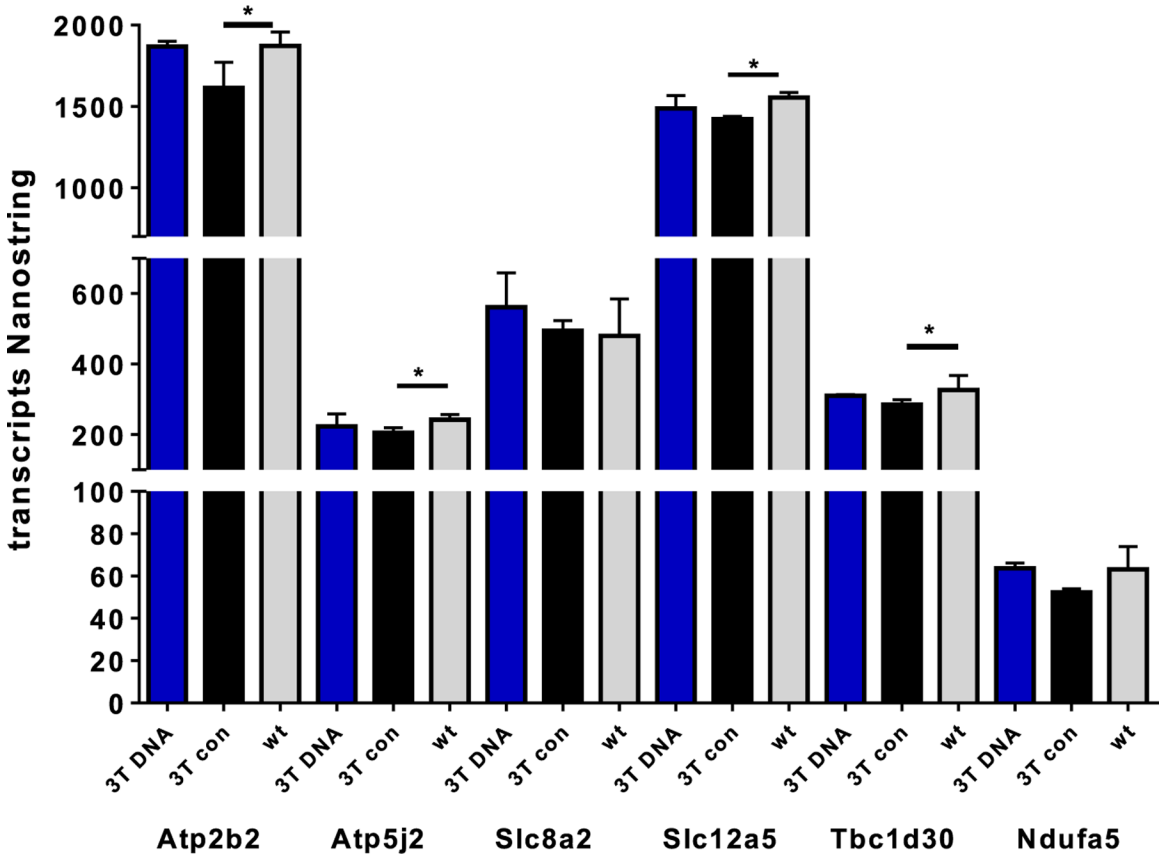

Fig. 8.

Transcript levels of six genes involved in vesicle formation trafficking analyzed with the mouse AD gene panel. A) Comparison of transcript numbers for the genes *Atp2b2* (ATPase, Ca++ transporting, plasma membrane 2), *Atp5j2* (ATP synthase, H+ transporting, mitochondrial F0 complex, subunit F2), *Slc8a2* (solute carrier family 8 (sodium/calcium exchanger), member 2), *Slc12a5* (solute carrier family 12, member 5), *Tbc1d30* (TBC1 domain family, member 30), *and Ndufa5* (NADH:ubiquinone oxidoreductase subunit A5), in DNA Aβ42 immunized 3xTg-AD mouse brains (blue bars, n = 4), non-immunized 3xTg-AD mouse brain controls (black bars, n = 4), and wild-type controls (grey bars, n = 4). Shown are the median values with interquartile range, * indicates *p* values of <0.05, Kruskal-Wallis test.

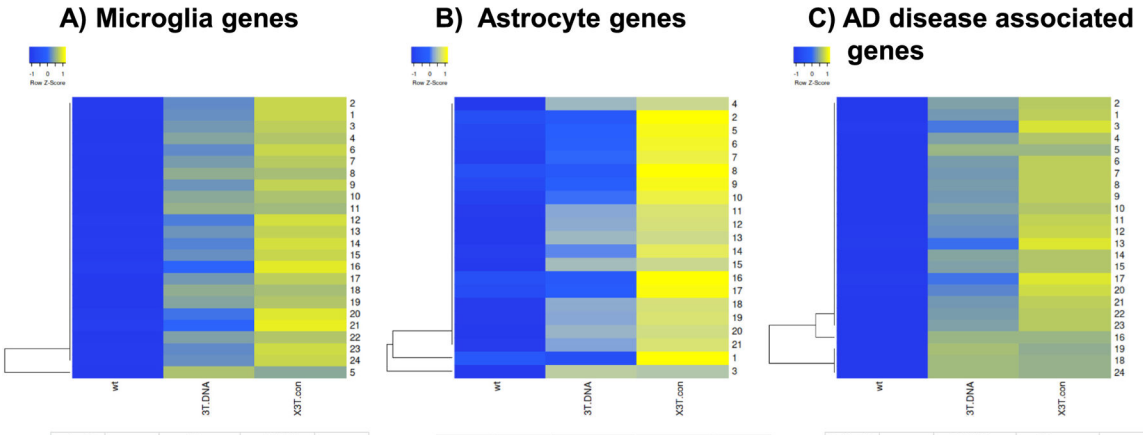

Probe Name	wt	3T con	3T DNA	
Abcc3	0	0.30103	0.2201081	1
C3	0	0.519828	0.365488	2
C3ar1	0	0.4377506	0.3424227	3
Ccl3	0	0.4031205	0.350248	4
Ccl4	0	0.392697	0.4313638	5
Cd68	0	0.5263393	0.376577	6
Cst7	0	0.5118834	0.421604	7
Ctse	0	1.242293	1.158363	8
Ctss	0	0.3541084	0.2648178	9
Fcrls	0	0.8260748	0.7520484	10
Gpr84	0	0.3201463	0.307496	11
Hcar2	0	0.3117538	0.1986571	12
Igf1	0	0.3180633	0.2405493	13
Itgax	0	0.3961994	0.2600714	14
Lilrb4a	0	0.6354837	0.4668676	15
Mmp12	0	0.5831988	0.2988531	16
Ptpn6	0	0.3117538	0.2455127	17
Slamf9	0	0.3201463	0.2944662	18
Spint1	0	0.3117538	0.269513	19
Spp1	0	0.363612	0.2121876	20
Tlr2	0	0.3747483	0.1875207	21
Tlr7	0	0.350248	0.2966652	22
Trem2	0	0.5037907	0.350248	23
Tyrobp	0	0.4683473	0.3384565	24

Probe Name	wt	3T DNA	3T con	
Agt	0	-0.01772878	0.09342169	1
C4a	0	0.08278538	0.4517864	2
Cd109	0	0.3944517	0.3838154	3
Cd14	0	0.4313638	0.5078559	4
Cp	0	0.05307844	0.1335389	5
Csf1	0	0.05307844	0.1271048	6
Fbln5	0	0.1105897	0.2201081	7
Fkbp5	0	0.02118928	0.1673174	8
Hspb1	0	0.1038037	0.2878017	9
Lcn2	0	0.2304489	0.4313638	10
Osmr	0	0.3201463	0.4393327	11
Psmb8	0	0.09691002	0.1271048	12
Ptx3	0	0.2741579	0.3304138	13
S100a10	0	0.08990512	0.1492191	14
S1pr3	0	0.2966652	0.346353	15
Serpina3n	0	0.0293838	0.2253093	16
Serping	0	0.05307844	0.1903317	17
Sox9	0	0.06445798	0.08635984	18
Srgn	0	0.1875207	0.2552725	19
Tgm1	0	0.4297523	0.5378191	20
Vim	0	0.303196	0.4232459	21

Probe Name	wt	3T DNA	3T con	
A2m	0	0.30103	0.3802113	1
Ahnak	0	0.07554698	0.08990512	2
Apoe	0	0.1335389	0.2174839	3
Arpc1b	0	0.2278867	0.269513	4
B2m	0	0.1986571	0.2013971	5
C1qa	0	0.3579348	0.4440448	6
C1qb	0	0.2922561	0.3692159	7
C1qc	0	0.2944662	0.3673559	8
Cldn5	0	0.1105897	0.1430148	9
Ctss	0	0.2922561	0.3424227	10
Cyba	0	0.252853	0.3304138	11
Fcer1g	0	0.2600714	0.3579348	12
Fn1	0	0.1238517	0.2227165	13
Grn	0	0.1492191	0.1731863	14
Laptm5	0	0.1760913	0.2068259	15
Plp1	0	0.1172713	0.1172713	16
S100a11	0	0.1430148	0.2479733	17
Slc39a1	0	0.1367206	0.1335389	18
Tgfbr1	0	0.1492191	0.1398791	19
Tgm2	0	0.120574	0.1760913	20
Tnfrsf1a	0	0.1643529	0.2121876	21
Trem2	0	0.3617278	0.4393327	22
Tyrobp	0	0.3324385	0.4014005	23
Zfp36	0	0.2121876	0.20412	24

Fig. 9.

Comparison of heat maps constructed for selected genes involved in microglial activation (A), astrocyte function (B), and genes classified as AD disease associated (C). The three columns in each of the graphs represent the three mouse groups tested, wild-type mice (wt, n = 4), DNA Aβ42 immunized 3xTg-AD (3 T DNA, n = 4), and non-immunized 3xTg-AD (3 T con, n = 4), with mean log2 ratio values of four brain samples in each of these groups. Tables below the heat maps list the genes and log2 ratios used for the assay in alphabetical order. Numbers in the last columns of the tables correspond to the numbers on the right hand side of the heat maps allowing for finding changes in the respective genes.

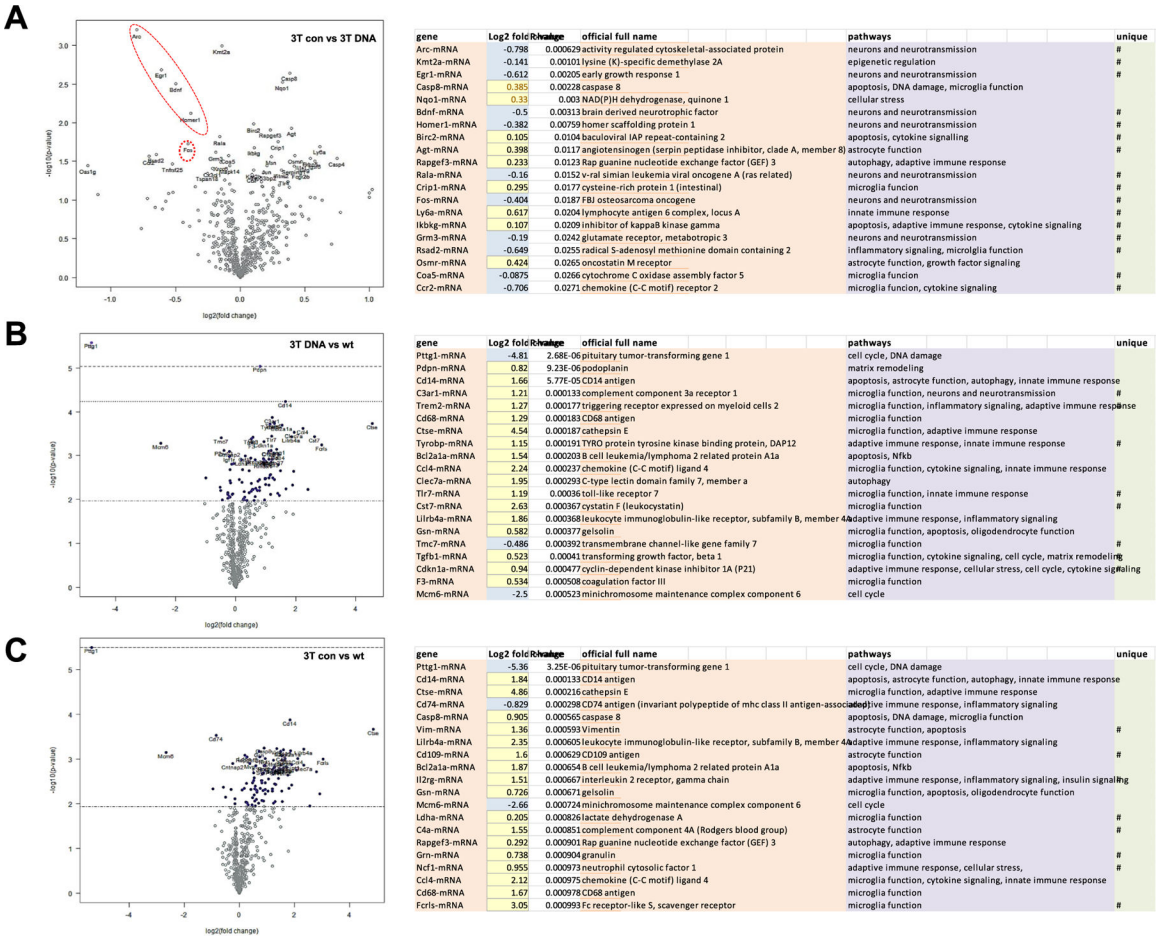

gene	Log2 fold change	p-value	official full name	pathways	unique
Arc-mRNA	-0.798	0.000629	activity regulated cytoskeletal-associated protein	neurons and neurotransmission	#
Kmt2a-mRNA	-0.141	0.00101	lysine (K)-specific demethylase 2A	epigenetic regulation	#
Egr1-mRNA	-0.612	0.00205	early growth response 1	neurons and neurotransmission	#
Casp8-mRNA	0.385	0.00228	caspase 8	apoptosis, DNA damage, microglia function	
Nqo1-mRNA	0.33	0.003	NAD(P)H dehydrogenase, quinone 1	cellular stress	
Bdnf-mRNA	-0.5	0.00313	brain derived neurotrophic factor	neurons and neurotransmission	#
Homer1-mRNA	-0.382	0.00759	homer scaffolding protein 1	neurons and neurotransmission	#
Birc2-mRNA	0.105	0.0104	baculoviral IAP repeat-containing 2	apoptosis, cytokine signalling	#
Agt-mRNA	0.398	0.0117	angiotensinogen (serpin peptidase inhibitor, clade A, member 8)	astrocyte function	#
Rapgef3-mRNA	0.233	0.0123	Rap guanine nucleotide exchange factor (GEF) 3	autophagy, adaptive immune response	
Ral a-mRNA	-0.16	0.0152	v-ral simian leukemia viral oncogene A (ras related)	neurons and neurotransmission	#
Crip1-mRNA	0.295	0.0177	cysteine-rich protein 1 (intestinal)	microglia funcion	#
Fos-mRNA	-0.404	0.0187	FBJ osteosarcoma oncogene	neurons and neurotransmission	#
Ly6a-mRNA	0.617	0.0204	lymphocyte antigen 6 complex, locus A	innate immune response	#
Ikbkg-mRNA	0.107	0.0209	inhibitor of kappaB kinase gamma	apoptosis, adaptive immune response, cytokine signaling	#
Grm3-mRNA	-0.19	0.0242	glutamate receptor, metabotropic 3	neurons and neurotransmission	#
Rsad2-mRNA	-0.649	0.0255	radical S-adenosyl methionine domain containing 2	inflammatory signaling, microglia function	#
Osmr-mRNA	0.424	0.0265	oncostatin M receptor	astrocyte function, growth factor signaling	
Coa5-mRNA	-0.0875	0.0266	cytochrome C oxidase assembly factor 5	microglia funcion	#
Ccr2-mRNA	-0.706	0.0271	chemokine (C-C motif) receptor 2	microglia funcion, cytokine signaling	#

gene	Log2 fold change	p-value	official full name	pathways	unique
Pttg1-mRNA	-4.81	2.68E-06	pituitary tumor-transforming gene 1	cell cycle, DNA damage	
Pdpn-mRNA	0.82	9.23E-06	podoplanin	matrix remodeling	
Cd14-mRNA	1.66	5.77E-05	CD14 antigen	apoptosis, astrocyte function, autophagy, innate immune response	
C3ar1-mRNA	1.21	0.000133	complement component 3a receptor 1	microglia function, neurons and neurotransmission	#
Trem2-mRNA	1.27	0.000177	triggering receptor expressed on myeloid cells 2	microglia function, inflammatory signaling, adaptive immune response	
Cd68-mRNA	1.29	0.000183	CD68 antigen	microglia function	
Ctse-mRNA	4.54	0.000187	cathepsin E	microglia function, adaptive immune response	
Tyrobp-mRNA	1.15	0.000191	TYRO protein tyrosine kinase binding protein, DAP12	adaptive immune response, innate immune response	#
Bcl2a1a-mRNA	1.54	0.000203	B cell leukemia/lymphoma 2 related protein A1a	apoptosis, Nfkb	
Ccl4-mRNA	2.24	0.000237	chemokine (C-C motif) ligand 4	microglia function, cytokine signaling, innate immune response	
Clec7a-mRNA	1.95	0.000293	C-type lectin domain family 7, member a	autophagy	
Tlr7-mRNA	1.19	0.00036	toll-like receptor 7	microglia function, innate immune response	#
Cst7-mRNA	2.63	0.000367	cystatin F (leukocystatin)	microglia function	#
Lilrb4a-mRNA	1.86	0.000368	leukocyte immunoglobulin-like receptor, subfamily B, member 4A	adaptive immune response, inflammatory signaling	
Gsn-mRNA	0.582	0.000377	gelsolin	microglia function, apoptosis, oligodendrocyte function	
Tmc7-mRNA	-0.486	0.000392	transmembrane channel-like gene family 7	microglia function	#
Tgfb1-mRNA	0.523	0.00041	transforming growth factor, beta 1	microglia function, cytokine signaling, cell cycle, matrix remodeling	#
Cdkn1a-mRNA	0.94	0.000477	cyclin-dependent kinase inhibitor 1A (P21)	adaptive immune response, cellular stress, cell cycle, cytokine signaling	#
F3-mRNA	0.534	0.000508	coagulation factor III	microglia function	
Mcm6-mRNA	-2.5	0.000523	minichromosome maintenance complex component 6	cell cycle	

gene	Log2 fold change	p-value	official full name	pathways	unique
Pttg1-mRNA	-5.36	3.25E-06	pituitary tumor-transforming gene 1	cell cycle, DNA damage	
Cd14-mRNA	1.84	0.000133	CD14 antigen	apoptosis, astrocyte function, autophagy, innate immune response	
Ctse-mRNA	4.86	0.000216	cathepsin E	microglia function, adaptive immune response	
Cd74-mRNA	-0.829	0.000298	CD74 antigen (invariant polypeptide of mhc class II antigen-associated)	adaptive immune response, inflammatory signaling	
Casp8-mRNA	0.905	0.000565	caspase 8	apoptosis, DNA damage, microglia function	
Vim-mRNA	1.36	0.000593	Vimentin	astrocyte function, apoptosis	#
Lilrb4a-mRNA	2.35	0.000605	leukocyte immunoglobulin-like receptor, subfamily B, member 4A	adaptive immune response, inflammatory signaling	
Cd109-mRNA	1.6	0.000629	CD109 antigen	astrocyte function	#
Bcl2a1a-mRNA	1.87	0.000654	B cell leukemia/lymphoma 2 related protein A1a	apoptosis, Nfkb	
Il2rg-mRNA	1.51	0.000667	interleukin 2 receptor, gamma chain	adaptive immune response, inflammatory signaling, insulin signaling	
Gsn-mRNA	0.726	0.000671	gelsolin	microglia function, apoptosis, oligodendrocyte function	
Mcm6-mRNA	-2.66	0.000724	minichromosome maintenance complex component 6	cell cycle	
Ldha-mRNA	0.205	0.000826	lactate dehydrogenase A	microglia function	#
C4a-mRNA	1.55	0.000851	complement component 4A (Rodgers blood group)	astrocyte function	#
Rapgef3-mRNA	0.292	0.000901	Rap guanine nucleotide exchange factor (GEF) 3	autophagy, adaptive immune response	
Grn-mRNA	0.738	0.000904	granulin	microglia function	#
Ncf1-mRNA	0.955	0.000973	neutrophil cytosolic factor 1	adaptive immune response, cellular stress,	#
Ccl4-mRNA	2.12	0.000975	chemokine (C-C motif) ligand 4	microglia function, cytokine signaling, innate immune response	
Cd68-mRNA	1.67	0.000978	CD68 antigen	microglia function	
Fcrls-mRNA	3.05	0.000993	Fc receptor-like S, scavenger receptor	microglia function	#

Fig. 10.

Scatterplots showing the most significant differently expressed genes (out of 750 genes tested in the Neuroinflammation gene panel) in the comparison of 3 T controls vs 3 T DNA (A), 3 T DNA vs wt (B), and 3 T controls vs wt (C). The scatterplots (left hand side of the graph) show statistical significance (log10 *p* value) versus magnitude of change (log2 fold change) for a visual identification of genes with large fold changes that are also statistically significant and may be the most biologically significant genes. In these volcano plots, the most upregulated genes are towards the right, the most downregulated genes are towards the left, and the most statistically significant genes are towards the top (top two quadrants, down-regulated, and upregulated). The lower two quadrants contain all the differently expressed genes (lower left, lower right) which do not reach high significance in this particular assay and are the majority of genes which do not show significant differences in the comparison of the two groups (major drop). Tables on the right hand side of the graph list the Top 20 most significant differently expressed genes. Values in the log2 change row are highlighted as downregulated in blue or upregulated in yellow. Each set of comparison has a number of genes which are unique for this specific comparison (indicated with # in the last row of the table). B and C have genes involved in microglia function and inflammatory signaling, while the comparison in A has a large number of genes involved in neuronal pathways (7 of 20), which is unique for this set of genes. Immediate early genes stand out in

this comparison and are indicated with red circles. Values from 4 mice per group per used for the statistical analyses shown.

Table 1

Differently expressed genes in mouse brains, ≥1.4 fold ratio only (Mouse Neuroinflammation panel).

Transcript number significantly * higher in non-treated 3xTg-AD mice compared to wild-type controls and different in the two groups of AD mice **	***Abcc3,*** *Atf3,* ***Btk, C1qa, C1qb, C1qc, C3, C3ar1, C4a, Casp4,*** *Casp6,* ***Casp8, Ccl3,*** *Cx3cr1,* ***Cd109, Cd14, Cd244, Cd68, Cd72, Cd84, Ch25h, Clec7a,*** *Csf1, Csf3r, Cst7,* ***Ctse, Ctss,*** *Dock2, Fbnl5,* ***Fcer1g, Fcgr2b,*** *Fcgr3,* ***Gpr84,*** *Grn, Gsn,* ***Hcar2,*** *Hmox1, Hspb1, Ifi30, Igsf6, Il1r1,* ***Il2rg,*** *Il3ra, Il6ra, Inpp5d, Irak4, Irf8,* ***Itgax, Lilrb4a, Ly9,*** *Mafb,* ***Mmp12,*** *Mobbp,* ***Mpeg1, Msr1,*** *Ncf1, Ncr1,* ***Osmr,*** *Pik3cg,* ***Ptpn6, Ptprc,*** *Socs3, Srgn, Syk, Tgfb1,* ***Tgm1, Tlr2, Tlr7,*** *Tnfrsf1a, Tnfrsf1b,* ***Trem2, Tyrobp,*** *Vav1,* ***Vim***
Transcript number significantly higher in both groups of 3xTg-AD mice compared to wild-type controls	***Bcl2a1a,*** *Cdkn1a, Csfr1. F3, Gpr183, Itgb5,* ***Olfml3,*** *Pdpn,* ***S1pr3, Slamf9,*** *Tmem37*
Transcript number significantly lower in both groups of 3xTg-AD mice compared to wild-type controls	***Ercc2, Mcm6, Pttg1, Sln8, Ccl4***
Transcript number significantly higher in DNA Aβ42 immunized 3xTg-AD mice	*Lrcc25, Maff, Oas1g, Osgin1*
Transcript number significantly lower in non-immunized 3xTg-AD mice and levels similar to wild-type mouse brains in the DNA Aβ42 immunized 3xTg-AD mice ***	*Arc, Bdnf, Egr1, Kmt2a, Rala,*

Genes highlighted in bold had ratios ≥2.

* Significance between groups was analyzed using the non-parametric Kruskal-Wallis one-way analysis of variances including Dunn's posthoc test, p values <0.05 were stated as significant.

** Transcript levels were lower in the DNA Aβ42 immunized mice consistent with changes due to immunotherapy.

*** Genes in this group do not have the 1.4 ratio difference threshold, as these genes are expressed at lower levels in the non-immunized 3xTg-AD mice than in the wild-type controls.

Table 2

Differently expressed genes in mouse brains (Mouse AD panel).

Transcript number significantly * higher in non-treated 3xTg-AD mice compared to wild-type controls and different in the two groups of AD mice **	*A2m, Adipor2, Anin, Apoe, Arpc1b,* **C1qa, C1qb, C1qc,** *Cd63, Cldn11, Cldn5,* **Ctss, Cyba,** *Daam2, Dync2li1, Elovl1, Itgb5, Fam129b,* **Fcr1g,** *Fn1,* **Fxyd5,** *Gng12, Grn, Lamp2, Laptm5, Map7, Myh9, Myo1e, Nde1, Nrk2, Prelp, Prex2,* **Pros1,** *Rab31, Rin2, S100a11, Srgn, Tnfrsf1a, Tppp3, Trappc6a, Trem2, Tyrobp*
Transcript number significantly lower in non-treated 3xTg-AD mice compared to wild-type controls	*Amot, Atp2b2, Atp5j2, Car10, Cd47, Cd74, Chrm3, Chmb2, Cntnap2, Cor2a, Foxn2, Gdap1l1, Gpc1, Kcnip4, Kif13b, Per1, Pi4ka, Serpinb1a, Slc12a5, Stx1b, Stxbp1, Sult4a1, Tbc1d30, Tbc1d9, Tshz1, Vgf, Zmiz2*
Transcript number significantly higher in both groups of 3xTg-AD mice compared to wild-type controls	*B2m, Bmpr1b, Ctnnd1, Ermn, Fam189a2, H2afz, Lrp4, Mbp, Mog, Plp1, ScIt1, Sez612, Slc39a1, Tatdn3, Tgfbr1, Zfp36*
Transcript number significantly lower in both groups of 3xTg-AD mice compared to wild-type controls	*Bdh1, Cp1x1, Cyfip2, Dam1*
Transcript number significantly higher in DNA Aβ42 immunized 3xTg-AD mice ***	*Aldh7a1, Enpp2, Fam171a1, Pla2g16, Sub1, Yap1*
Transcript number significantly lower in DNA Aβ42 immunized 3xTg-AD mice	*Rras, Trappc2l*

Genes highlighted in red are classified as AD disease associated, genes shown in bold letters have a 2-fold expression difference to wild-type levels.

* Significance between groups was analyzed using the non-parametric Kruskal-Wallis one-way analysis of variances including Dunn's posthoc test, p values <0.05 were stated as significant.

** All of these genes have lower transcript numbers in the DNA Aβ42 immunized 3xTg-AD mice.

*** All of these genes have higher transcript numbers in the DNA Aβ42 immunized 3xTg-AD mice.